Biochemical and Biophysical Research Communications 441 (2013) 42–46

Contents lists available at ScienceDirect

Biochemical and Biophysical Research Communications

journal homepage: www.elsevier.com/locate/ybbrc

FABP3 and brown adipocyte-characteristic mitochondrial fatty acid oxidation enzymes are induced in beige cells in a different pathway from UCP1

Yuki Nakamura, Takahiro Sato, Yuki Shiimura, Yoshiki Miura, Masayasu Kojima *

Department of Molecular Genetics, Institute of Life Science, Kurume University, 1-1 Hyakunen-kouen, Kurume 839-0864, Japan

ARTICLE INFO

Article history:
Received 30 September 2013
Available online 12 October 2013

Keywords:
Brown adipocyte
White adipocyte
Beige cell/brite cell/recruitable brown fat cell
Heart-type fatty acid binding protein/fatty acid binding protein 3
Fatty acid oxidation

ABSTRACT

Cold exposure and β_3-adrenergic receptor agonist (CL316,243) treatment induce the production of beige cells, which express brown adipocytes(BA)-specific UCP1 protein, in white adipose tissue (WAT). It remains unclear whether the beige cells, which have different gene expression patterns from BA, express BA-characteristic fatty acid oxidation (FAO) proteins. Here we found that 5 day cold exposure and CL316,243 treatment of WAT, but not CL316,243 treatment of primary adipocytes of C57BL/6J mice, increased mRNA levels of BA-characteristic FAO proteins. These results suggest that BA-characteristic FAO proteins are induced in beige cells in a different pathway from UCP1.

1. Introduction

Two types of adipose tissue are found in mammals: white and brown. White adipose tissue (WAT) is highly adapted to store excess energy in the form of triglycerides. Conversely, brown adipose tissue (BAT) oxidizes chemical energy to produce heat in response to cold exposure. Uncoupling protein-1 (UCP1) and fatty acids play an important role in thermogenesis in BAT. UCP1 is specifically expressed in BAT and is localized to the inner membrane of the mitochondria. Its physiological role is to uncouple oxidative phosphorylation so that most of the energy is dissipated as heat rather than being converted to ATP. Fatty acids also play a key role in thermogenesis as the source of oxidative fuel in the mitochondria.

Compared to white adipocytes (WA), brown adipocytes (BA) contain different types of proteins involved in fatty acid oxidation (FAO). These differences appear to reflect functional differences in the two types of adipose tissue. For example, the expression of fatty acid binding protein 3 (FABP3) is dramatically enhanced in acute cold exposure and is thought to be essential for FAO in BAT; in contrast, FABP3 expression is negligible in WAT [1–3]. FABP3 is a member of the fatty acid binding protein family, which consists of 14–15 kDa intracellular proteins that reversibly bind to hydrophobic ligands, such as saturated and unsaturated long-chain fatty acids, with high affinity. FABPs act as lipid "chaperones" that have been implicated in fatty acid uptake, transport, and targeting [4]. Among these families, FABP3 in BA is thought to transport and deliver fatty acids to the mitochondria for oxidation. Fatty acids delivered to the mitochondria are β-oxidized by mitochondrial enzymes. Proteomic analyses of mitochondria from brown and white adipocytes revealed that their proteomes are considerably different, both qualitatively and quantitatively, and are further characterized by tissue-specific protein isoforms [5]. It has been shown that BA, compared with WA, express characteristic mitochondrial FAO enzyme isoforms such as acyl-Coenzyme A (acyl-CoA) synthetase short-chain family member 1 (ACSS1), acyl-CoA synthetase long-chain family member 5 (ACSL5), carnitine palmitoyltransferase 1b (CPT1b), long-chain acyl-CoA dehydrogenase (ACADL),

Abbreviations: WAT, white adipose tissue; BAT, brown adipose tissue; UCP1, uncoupling protein 1; WA, white adipocyte; BA, brown adipocyte; FAO, fatty acid oxidation; FABP3, fatty acid binding protein3/heart-type fatty acid binding protein; Acyl-CoA, acyl-Coenzyme A; ACSS1, acyl-CoA synthetase short-chain family member 1; ACSL5, acyl-CoA synthetase long-chain family member 5; CPT1b, carnitine palmitoyltransferase 1b; ACADL, long-chain acyl-Coenzyme A dehydrogenase; ACADM, medium-chain acyl-Coenzyme A dehydrogenase; ACADS, short-chain acyl-Coenzyme A dehydrogenase; ACAA2, 3-oxoacyl-Coenzyme A thiolase; β_3AR, β_3-adrenergic receptor; cAMP, cyclic AMP; CL, CL316,243; mRNA, messenger RNA; subWAT, subcutaneous WAT; i.p, intraperitoneal; SV, stromal-vascular; cDNA, complementary DNA; Rps18, ribosomal protein S18; PPAR, peroxisome proliferator-activated receptor; PGC-1, PPARγ coactivator 1.

* Corresponding author. Fax: +81 942 31 5212.
E-mail addresses: kojima_masayasu@kurume-u.ac.jp, nakamura_yuuki@med.kurume-u.ac.jp (M. Kojima).

0006-291X/$ - see front matter © 2013 Elsevier Inc. All rights reserved.
http://dx.doi.org/10.1016/j.bbrc.2013.10.014

medium-chain acyl-CoA dehydrogenase (ACADM), short-chain acyl-CoA dehydrogenase (ACADS), and 3-oxoacyl-CoA thiolase (ACAA2). Defects in the *Acadl* or *Acads* gene of mice resulted in an inability to maintain body temperature under cold conditions [6], which suggests that mitochondrial FAO enzymes play a vital role in thermogenesis. Fatty acids delivered to the mitochondria are activated to fatty acyl-CoAs by acyl-CoA synthetases such as ACSS1 and ACSL5. Once activated, long-chain fatty acids require carnitine palmitoyltransferase, including CPT1b, to be transported into mitochondrial matrix. In the matrix space, acyl-CoA dehydrogenases such as ACADL, ACADM and ACADS, and ACAA2 catabolize acyl-CoAs, which are ultimately processed to produce acetyl-CoAs. Thereafter, acetyl-CoAs enter the citric acid cycle and electron transport chain.

Recently, it has been reported that brown fat-like adipocytes having a multilocular morphology and expressing the BA-specific UCP1 protein exist within certain WATs in mice and rats [7]. These cells have been called recruitable brown fat cells, brown in white (brite) cells, or beige cells [8], and they become more prominent upon prolonged stimulation by cold or β_3-adrenergic receptor (β_3AR) agonists such as CL316,243 (CL) that elevate intracellular cyclic AMP (cAMP) [9]. This brown-like transformation of WAT is the most notable in the inguinal subcutaneous depot [10]. The gene expression pattern and origin of beige cells have been reported to be distinct from those of BA [11,12]. However, it has not been well documented whether BA-characteristic FAO proteins are up-regulated in beige cells.

In this study, using C57BL/6J mice, we demonstrated that cold exposure or β_3AR agonist treatment increased messenger RNA (mRNA) and protein expression of FABP3 and increased mRNA levels of several BA-characteristic mitochondrial FAO enzymes in subcutaneous WAT (subWAT). In addition, using primary adipocytes isolated from subWAT, we examined the effect of a β_3AR agonist or cAMP enhancer on the expression of these proteins in adipocytes. Unexpectedly, our results suggest that these BA-characteristic FAO proteins are induced in a different pathway from UCP1.

2. Materials and methods

2.1. Animals

C57BL/6J mice (4 or 8 weeks old, CLEA Japan, Tokyo, Japan) were fed standard rodent chow pellets and water *ad libitum* and were housed at 23 ± 1 °C on a 12 h light/dark cycle. All experimental procedures were conducted in compliance with protocols approved by the Ethical Committee for the Research of Life Science in Kurume University.

2.2. Cold exposure and β_3-adrenergic receptor agonist (CL316,243) treatment in vivo

Eight-week-old male mice were fed standard rodent chow pellets and water *ad libitum*. The mice were housed individually in plastic cages and divided into two groups that were counterbalanced by body mass. For the cold exposure studies, control groups were maintained at 23 ± 1 °C, whereas cold exposure groups were maintained at 4 °C for 5 days. For the CL treatment studies, control groups were injected intraperitoneally (i.p) once daily with saline (200 μl) for 5 days, whereas CL treatment groups were injected i.p once daily with CL (1 mg/kg; Tocris Bioscience, Bristol, UK) in saline (200 μl) for 5 days. After the mice were killed by decapitation, their posterior subcutaneous fat pads (inguinal-dorsolumbar portion) were separated immediately and used for subsequent processing and analyses.

2.3. Adipose tissue fractionation

Adipose tissue was divided into adipocyte and stromal-vascular (SV) fractions. Freshly excised subcutaneous fat pads from 8-week-old male C57BL/6J mice were rinsed in PBS, minced with scissors, and digested with 3 mg/ml collagenase type II (Worthington, Lakewood, NJ, USA) in isolation buffer (123 mM NaCl, 5 mM KCl, 1.3 mM $CaCl_2$, 5 mM glucose, 100 mM HEPES, and 4% BSA, pH 7.4) for 1 h at 37 °C. The digested tissue was filtered through a 200 μm nylon mesh to remove undigested tissue and centrifuged at 210×*g* for 1 min. The mature adipocytes floated to the surface, and the SV cells (capillary, endothelial, mast, macrophage, and epithelial cells) were deposited. The floating cells and the SV cells were washed twice with the isolation buffer, recentrifuged at 210×*g*, and collected as the mature adipocytes and SV cells, respectively. Total RNA from the mature adipocytes and SV cells was isolated using TRIzol (Life Technologies Corporation, Carlsbad, CA) reagent. Adequate separation of adipocytes and SV cells was confirmed by RT-PCR for the adipocyte markers *adiponectin* and *Ucp1* and the SV cell marker *Ucp2* (data not shown).

2.4. Quantitative RT-PCR analysis

Total RNA from mouse tissues or cultured cells was isolated using the TRIzol method combined with RNeasy mini columns (QIAGEN, Valencia, CA) according to the manufacturer's instructions. For quantitative RT-PCR, 0.5–1 μg of total RNA was used to synthesize complementary DNA (cDNA). Target cDNA levels were quantified by real-time PCR by using the ABI PRISM 7000 sequence detection system (Applied Biosystems, Foster City, CA) with SYBR Green (Applied Biosystems). Relative mRNA expression levels were calculated using mouse ribosomal protein S18 (*Rps18*). The primer sequences were as follows: *Acaa2* (forward: 5′-ggctctggtttccagtccatc-3′ ; reverse: 5′-gaagcgcacatttctgacacagta-3′), *Acadl* (forward: 5′-ctacctcatgcaagagcttccaca-3′; reverse: 5′-cttcaaacatgaactcacaggcaga-3′), *Acadm* (forward: 5′-tgatgtggcggccattaaga-3′; reverse: 5′-gggttagaacgtgccaacaagaa-3′), *Acads* (forward: 5′-aagtttggatccgcacagcag-3′; reverse: 5′-caagctttggtgccgttgag-3′), *Acsl5* (forward: 5′-cattcggcgggacagtttg-3′; reverse: 5′-atcccattgcagccctgaag-3′), *Acss1* (forward: 5′-agatcctgaagactctgcctgtcc-3′; reverse: 5′-ttgcatcactcaccaatgtcca-3′), *Cpt1b* (forward: 5′-gagacaggacactgtgtgggtga-3′; reverse: 5′-tggtacgagttctcgatggcttc-3′), *Fabp3* (forward: 5′-tggctagcatgaccaagcctactac-3′; reverse: 5′-gttccacttctgcacatggatga-3′), *Rps18* (forward: 5′-ttctggccaacggtctagacaac-3′; reverse: 5′-ccagtggtcttggtgtgctga-3′), and *Ucp1* (forward: 5′-gggcattcagaggcaaatcag-3′; reverse: 5′-ctgccacacctccagtcattaag-3′).

2.5. ELISA

Tissue concentrations of FABP3 protein were measured using a sandwich-type ELISA (Hycult Biotechnology, Uden. The Netherlands) according to the manufacturer's protocol. The values were normalized to the total protein concentrations determined by the bicinchoninic acid protein assay (Pierce, Rockford, IL).

2.6. Primary cell culture and treatment

For the culture of primary subcutaneous white adipocytes, posterior subcutaneous fat pads (inguinal-dorsolumbar portion) were isolated from 4-week-old C57BL/6J male mice. The isolated tissues were rinsed in PBS, minced with scissors, and digested with 1 mg/ml collagenase type II (Worthington) in isolation buffer at 37 °C for 30 min. Cell suspensions were filtered through a 100 μm filter and centrifuged at 210×*g* for 10 min. The pellet consisting of preadipocytes was resuspended in 1 mL of red blood cell lysis buffer (IBL, Gunma, Japan). After incubation for 3 min at

room temperature, 10 ml plating medium (Dulbecco's modified Eagle's medium supplemented with ascorbate, biotin, pantothenate, triiodothyronine, octanoic acid, penicillin–streptomycin, and FCS from a white adipocyte culture kit [TaKaRa Bio, Shiga, Japan]) was added to the cell suspension. To remove endothelial cell clumps, the cell suspension was filtered through a sterile 20 μm mesh filter. Preadipocytes were recovered by centrifugation and washed in plating medium twice. The preadipocytes were then plated on 12-well tissue culture plates at a density of 8×10^4 cells/cm^2 in plating medium and cultured at 37 °C under a humidified atmosphere of 95% air and 5% CO_2. The medium was changed on day 1 and then every second day. Induction of differentiation was performed using differentiation medium (plating medium supplemented with insulin, dexamethasone, and 3-isobutyl-L-methylxanthin [TaKaRa Bio]) for 2 days. Subsequently, cells were cultured in maintenance medium (plating medium supplemented with insulin [TaKaRa Bio]) for 8 days. The cells were incubated in serum-free medium for 12 h prior to harvest of cultures, and the cultures were treated with or without 1 μM CL or 10 μM forskolin for 6 h prior to harvesting.

2.7. Statistical analysis

All experimental data are presented as the mean ± SE. Comparisons were performed by two-tailed *t*-tests. The criterion for statistical significance was $p < 0.05$ for all tests (Graph Pad PRISM 5.0a; Graph Pad Software Inc., La Jolla, CA).

3. Results

3.1. Cold exposure and β_3-adrenergic receptor agonist (CL316,243) treatment induced gene expression of Fabp3 and BA-characteristic mitochondrial fatty acid oxidation enzymes in subcutaneous WAT in vivo

To confirm the browning of WAT after 5-day cold exposure (4 °C) or CL treatment, we studied *Ucp1* mRNA expression in subWAT by using quantitative RT-PCR. Both 5-day cold exposure and CL treatment significantly induced *Ucp1* mRNA expression (Fig. 1A). As expected, brown-like transformation of subWAT occurred after both 5-day cold exposure and CL treatment.

FABP3 is essential for fatty acid oxidation in BAT, whereas its expression is negligible in WAT [1–3]. To examine the effects of cold exposure or CL treatment on FABP3 expression, we investigated *Fabp3* mRNA expression in subWAT. Cold exposure and CL treatment markedly increased *Fabp3* mRNA expression by 102-fold and 22-fold, respectively compared to the control ($p < 0.01$, Fig. 1B).

WAT is composed of mature adipocytes and the SV fraction. To determine which cell populations in subWAT express FABP3, we measured *Fabp3* mRNA levels in fractionated adipose tissue. Fractionation of WAT by centrifugation showed that *Fabp3* was mainly expressed in mature white adipocytes rather than in the SV fraction, after both cold exposure and CL treatment (Fig. 1B).

Furthermore, we analyzed the content of protein by using a FABP3 immunoassay, which showed that cold exposure and CL

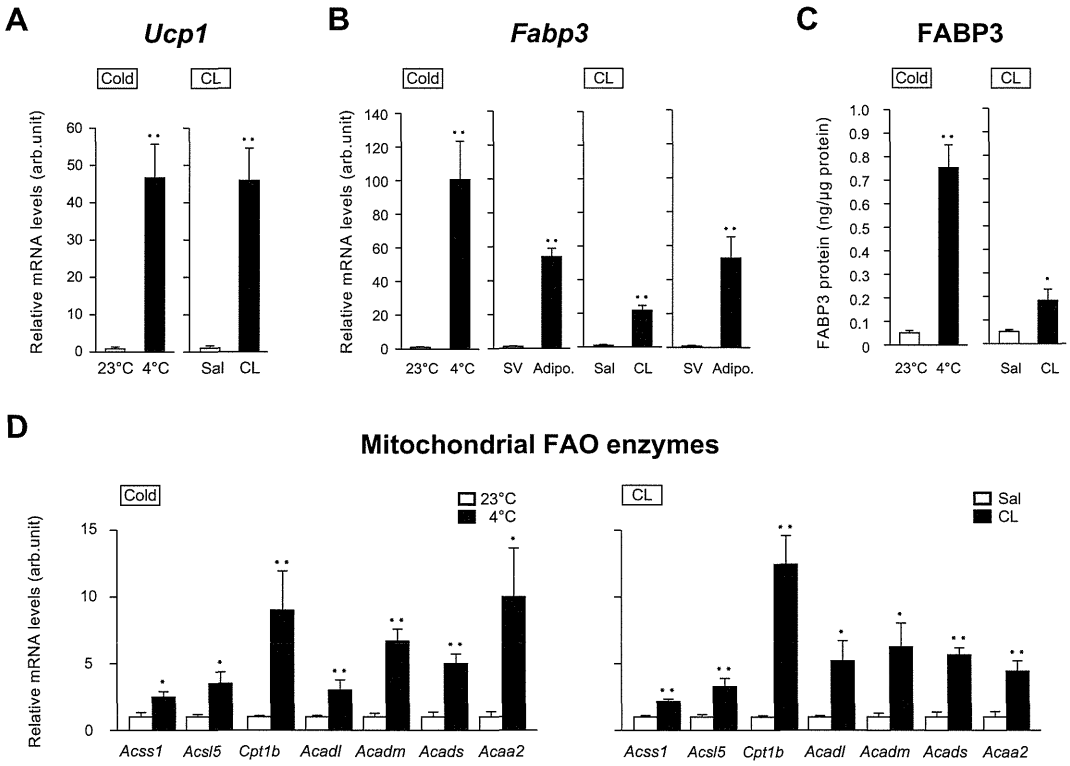

Fig. 1. Cold exposure and β_3-adrenergic receptor agonist (CL316,243) treatment induced gene expression of *Fabp3* and BA-characteristic mitochondrial FAO enzymes in subcutaneous white adipose tissue. C57BL/6J mice at 8 weeks of age maintained at 23 °C or 4 °C for 5 days. (A–D, left panels) C57BL/6J mice at 8 weeks of age were injected i.p once daily with saline (Sal) or CL316,243 in saline (CL) for 5 days. (A–D, right panels) The subcutaneous fat pads of the mice were used for the following analyses. (A) *Ucp1* mRNA levels in subcutaneous white adipose tissues (subWAT). (B) *Fabp3* mRNA levels in subWAT and the adipocyte fraction (Adipo.) compared to the stromal-vascular fraction (SV) of subWAT. (C) FABP3 protein concentrations in subWAT determined by an immunoassay. Values are expressed as nanograms of FABP3 per microgram of total cellular protein. (D) mRNA levels of BA-characteristic mitochondrial fatty acid oxidation (FAO) enzymes (*Acss1*, *Acsl5*, *Cpt1b*, *Acadl*, *Acadm*, *Acads*, and *Acaa2*) in subWAT. Gene expression was determined by real-time RT-PCR and normalized against 18S rRNA levels. In all panels, values represent the means ± SE ($n = 4–5$). $^*p < 0.05$, $^{**}p < 0.01$.

treatment increased the content of FABP3 protein by 14-fold and 3-fold, respectively, compared to the control ($p < 0.01$ and $p < 0.05$, respectively, Fig. 1C). Thus, FABP3 expression increases with the brown-like transformation of WAT.

The increased FABP expression in WAT implies that more fatty acids are transported to the mitochondria for oxidation. Fatty acids delivered to the mitochondria are β-oxidized by mitochondrial enzymes. We therefore investigated whether cold exposure or CL treatment increases the levels of BA-characteristic mitochondrial FAO enzymes in subWAT, and found that the mRNA levels of *Acss1*, *Acsl5*, *Cpt1b*, *Acadl*, *Acadm*, *Acads*, and *Acaa2* increased under both conditions (Fig. 1D).

3.2. CL316,243 or cAMP enhancer (forskolin) treatment did not induce the expression of Fabp3 or BA-characteristic mitochondrial FAO enzymes in primary adipocytes of subWAT

To investigate the direct effect of CL or a cAMP enhancer, forskolin, on the adipocytes of subWAT, we used a culture of primary adipocytes isolated from subWAT depots. CL or forskolin treatment for 6 h increased *Ucp1* mRNA expression by 29-fold and 39-fold, respectively, compared to the control ($p < 0.01$, Fig. 2A). These results suggest that *Ucp1* expression is induced by the β_3AR-cAMP pathway and that the primary adipocytes are beige cells.

It was previously reported that norepinephrine elevated the transcript level of FABP3 in primary brown adipocytes and a brown adipocyte cell line [1,2]. However, in beige cells, the effects of β_3AR agonists on the transcript level of FABP3 are not clear. To study whether FABP3 is induced by the β_3AR-cAMP pathway, we examined *Fabp3* mRNA expression following CL or forskolin treatment. CL or forskolin treatment for 6 h decreased the level of *Fabp3* mRNA (Fig. 2B).

Furthermore, we investigated the effect of CL or forskolin treatment on the mRNA levels of BA-characteristic mitochondrial FAO enzymes. CL or forskolin treatment for 6 h did not induce but rather reduced the mRNA levels of *Acss1*, *Acsl5*, *Cpt1b*, *Acadl*, *Acadm*, *Acads*, and *Acaa2* (Fig. 2C).

4. Discussion

It has been reported that beige cells that express UCP1 protein become more prominent within WAT in mice after cold exposure or β_3AR agonist treatment. The objective of this study was to determine whether FABP3 and BA-characteristic mitochondrial FAO enzymes are induced after brown-like transformation of WAT. We present evidence here that cold exposure or CL treatment increases mRNA and protein expression of FABP3 and increases mRNA levels of BA-characteristic mitochondrial FAO enzymes (ACSS1, ACSL5, CPT1b, ACADL, ACADM, ACADS, and ACAA2) in subWAT *in vivo*. In addition, using primary adipocytes, we showed that CL or forskolin treatment increased *Ucp1* mRNA expression; however, it did not change or decrease the mRNA expression of *Fabp3* and BA-characteristic mitochondrial FAO enzymes.

In BAT, the transcript levels of *Fabp3* and *Cpt1b* but not *Acadm* and *Acadl* are elevated by cold exposure [13]. These results suggest that regulation of *Fabp3* and *Cpt1b* expression is the rate-limiting step in FAO, and the constitutive expression of *Acadm* and *Acadl* is sufficient to enhance β-oxidation in BAT. Some reports have mentioned that the gene expression of *Cpt1b* is increased in WAT after cold exposure or CL treatment [14]. In this study, we found that the gene expression of not only *Cpt1b* but also *Fabp3*, *Acadm*, and *Acadl* was induced by cold exposure in subWAT. The constitutive expression of *Fabp3*, *Acadm*, and *Acadl* is lower in WAT than in BAT; therefore, the up-regulation of these genes is considered to be necessary to enhance β-oxidation with brown-like transformation

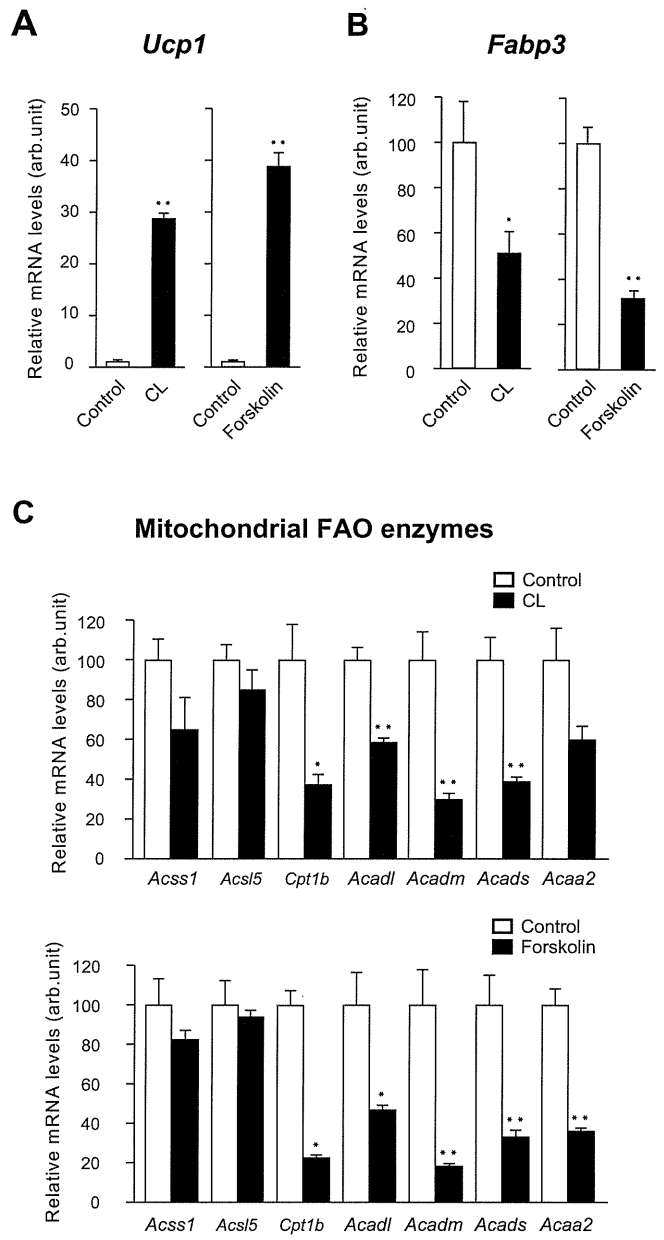

Fig. 2. β_3-adrenergic receptor agonist (CL316,243) or cAMP enhancer (forskolin) treatment did not induce gene expression of *Fabp3* and BA-characteristic mitochondrial FAO enzymes in primary adipocytes of subWAT. Primary adipocytes of subWAT were grown as described in Section 2 and used for the following analyses. Cells were pretreated for 6 h with or without 1 μM CL316,243 (CL) or 10 μM forskolin. Gene expression of *Ucp1* (A), *Fabp3* (B), and BA-characteristic mitochondrial FAO enzymes (*Acss1*, *Acsl5*, *Cpt1b*, *Acadl*, *Acadm*, *Acads*, and *Acaa2*) (C) was determined by real-time RT-PCR and normalized against 18S rRNA levels. In all panels, values represent the means ± SE ($n = 4$). $^{*}p < 0.05$, $^{**}p < 0.01$.

in WAT. Our findings suggest that BA-characteristic FAO proteins are inducible, and the increased levels of the proteins appear to reflect enhanced β-oxidation with brown-like transformation of WAT.

β_3AR is of pivotal importance in the brown-like transformation of WAT after cold exposure because β_3AR knockout mice show decreased occurrence of the brown-like transformation of WAT [15]. We showed that CL treatment increased the levels of FABP3 and BA-characteristic mitochondrial FAO enzymes in subWAT. By contrast, using primary adipocytes, we found that CL and forskolin treatment increased *Ucp1* mRNA expression but did not change or decrease the mRNA expression of *Fabp3* or BA-characteristic

mitochondrial FAO enzymes. Our culture experiments suggest that FABP3 and BAT-characteristic mitochondrial FAO enzymes are induced in a different pathway from UCP1 induction in beige cells.

Many genes involved in FAO have been shown to be induced by peroxisome proliferator-activated receptor α (PPARα) [16]. PPARα is a fatty acid-activated nuclear receptor and known to be an important regulator of mitochondrial β-oxidation in tissues such as the heart, liver, and BAT. However, the expression of PPARα in WAT is very low and its function remains unclear. It has been reported that ectopic overexpression of PPARα and PPARγ coactivator 1 (PGC-1) in adipocyte-like differentiated 3T3L-1 cells cooperatively induces the expression of mitochondrial FAO enzyme genes including *Acadm* and *Acadl* [17]. PGC-1 serves as a transcriptional coactivator in the control of mitochondrial FAO enzyme gene expression. We confirm that the *Ppara* mRNA level increases in subWAT after CL treatment *in vivo* as reported previously by Li et al. [18]. However, we found that the *Ppara* mRNA level was decreased in the primary adipocytes after CL treatment (data not shown). PPARα could be essential for the expression of several BAT characteristic proteins involved in FAO in subWAT. Although FABP3 is reported to augment the transcriptional activity of PPARα [19], the regulatory mechanism of *Ppara* expression in WAT remains unclear. Further studies are needed to uncover the molecular mechanism for the regulation and function of PPARα in WAT.

A limitation of our study is the heterogeneity of the primary adipocytes isolated from subWAT, as cellular heterogeneity was previously shown for clonal cells derived from the subWAT of mice [12]. Therefore, more precise isolation and purification of beige cells in subWAT are required for further investigation.

Elucidating the molecular mechanism involved in FAO in beige cells has important medical implications and may provide clues in the development of anti-obesity agents. Recent studies have shown that thermogenic UCP1-positive adipocytes exist in adult humans, and the most of these adipocytes in humans are molecularly similar to murine beige cells rather than brown adipocytes [12,20]. Modulation of the expression of BA-characteristic FAO proteins in beige cells may represent a novel therapeutic target for obesity and metabolic diseases.

In summary, we show that the expression of BA-characteristic FAO proteins is increased in subWAT after cold exposure or CL treatment. Moreover, primary culture experiments suggest that these proteins are induced in a different pathway from UCP1. Further investigation is necessary to determine the regulatory mechanism for the expression of BA-characteristic FAO proteins in subWAT.

Acknowledgments

We thank K. Oishi, Y. Shibata, and M. Yamane for their assistance. This work was supported by a Grant-in-Aid for Scientific Research (B) from the Ministry of Education, Culture, Sports, Science and Technology of Japan and grants from Research on Measures for Intractable Diseases from Health and Labour Sciences Research Grants, Subsides to Private Schools, the Vehicle Racing Commemorative Foundation, and Japan Foundation for Applied Enzymology.

References

[1] T. Daikoku, Y. Shinohara, A. Shima, N. Yamazaki, H. Terada, Dramatic enhancement of the specific expression of the heart-type fatty acid binding protein in rat brown adipose tissue by cold exposure, FEBS Lett. 410 (1997) 383–386.
[2] L. Vergnes, R. Chin, S.G. Young, K. Reue, Heart-type fatty acid-binding protein is essential for efficient brown adipose tissue fatty acid oxidation and cold tolerance, J. Biol. Chem. 286 (2011) 380–390.
[3] T. Yamamoto, A. Yamamoto, M. Watanabe, M. Kataoka, H. Terada, Y. Shinohara, Quantitative evaluation of the effects of cold exposure of rats on the expression levels of ten FABP isoforms in brown adipose tissue, Biotechnol. Lett. 33 (2011) 237–242.
[4] M. Furuhashi, G.S. Hotamisligil, Fatty acid-binding proteins: role in metabolic diseases and potential as drug targets, Nat. Rev. Drug Discov. 7 (2008) 489–503.
[5] F. Forner, C. Kumar, C.A. Luber, T. Fromme, M. Klingenspor, M. Mann, Proteome differences between brown and white fat mitochondria reveal specialized metabolic functions, Cell Metab. 10 (2009) 324–335.
[6] C. Guerra, R.A. Koza, K. Walsh, D.M. Kurtz, P.A. Wood, L.P. Kozak, Abnormal nonshivering thermogenesis in mice with inherited defects of fatty acid oxidation, J. Clin. Invest. 102 (1998) 1724–1731.
[7] P. Young, J.R. Arch, M. Ashwell, Brown adipose tissue in the parametrial fat pad of the mouse, FEBS Lett. 167 (1984) 10–14.
[8] J. Ishibashi, P. Seale, Beige can be slimming, Science 328 (2010) 1113–1114.
[9] J. Himms-Hagen, A. Melnyk, M.C. Zingaretti, E. Ceresi, G. Barbatelli, S. Cinti, Multilocular fat cells in WAT of CL-316243-treated rats derive directly from white adipocytes, Am. J. Physiol. Cell Physiol. 279 (2000) C670–C681.
[10] G. Barbatelli, I. Murano, L. Madsen, Q. Hao, M. Jimenez, K. Kristiansen, J.P. Giacobino, R. De Matteis, S. Cinti, The emergence of cold-induced brown adipocytes in mouse white fat depots is determined predominantly by white to brown adipocyte transdifferentiation, Am. J. Physiol. Endocrinol. Metab. 298 (2010) E1244–E1253.
[11] P. Seale, B. Bjork, W. Yang, S. Kajimura, S. Chin, S. Kuang, A. Scimè, S. Devarakonda, H.M. Conroe, H. Erdjument-Bromage, P. Tempst, M.A. Rudnicki, D.R. Beier, B.M. Spiegelman, PRDM16 controls a brown fat/skeletal muscle switch, Nature 454 (2008) 961–967.
[12] J. Wu, P. Boström, L.M. Sparks, L. Ye, J.H. Choi, A.H. Giang, M. Khandekar, K.A. Virtanen, P. Nuutila, G. Schaart, K. Huang, H. Tu, W.D. van Marken Lichtenbelt, J. Hoeks, S. Enerbäck, P. Schrauwen, B.M. Spiegelman, Beige adipocytes are a distinct type of thermogenic fat cell in mouse and human, Cell 150 (2012) 366–376.
[13] T. Daikoku, Y. Shinohara, A. Shima, N. Yamazaki, H. Terada, Specific elevation of transcript levels of particular protein subtypes induced in brown adipose tissue by cold exposure, Biochim. Biophys. Acta 1457 (2000) 263–272.
[14] A. Vegiopoulos, K. Müller-Decker, D. Strzoda, I. Schmitt, E. Chichelnitskiy, A. Ostertag, M. Berriel Diaz, J. Rozman, M. Hrabe de Angelis, R.M. Nüsing, C.W. Meyer, W. Wahli, M. Klingenspor, S. Herzig, Cyclooxygenase-2 controls energy homeostasis in mice by de novo recruitment of brown adipocytes, Science 328 (2010) 1158–1161.
[15] M. Jimenez, G. Barbatelli, R. Allevi, S. Cinti, J. Seydoux, J.P. Giacobino, P. Muzzin, F. Preitner, Beta 3-adrenoceptor knockout in C57BL/6J mice depresses the occurrence of brown adipocytes in white fat, Eur. J. Biochem. 270 (2003) 699–705.
[16] S. Mandard, M. Müller, S. Kersten, Peroxisome proliferator-activated receptor alpha target genes, Cell. Mol. Life Sci. 61 (2004) 393–416.
[17] R.B. Vega, J.M. Huss, D.P. Kelly, The coactivator PGC-1 cooperates with peroxisome proliferator-activated receptor alpha in transcriptional control of nuclear genes encoding mitochondrial fatty acid oxidation enzymes, Mol. Cell. Biol. 20 (2000) 1868–1876.
[18] P. Li, Z. Zhu, Y. Lu, J.G. Granneman, Metabolic and cellular plasticity in white adipose tissue II: role of peroxisome proliferator-activated receptor-alpha, Am. J. Physiol. Endocrinol. Metab. 289 (2005) E617–E626.
[19] N.S. Tan, N.S. Shaw, N. Vinckenbosch, P. Liu, R. Yasmin, B. Desvergne, W. Wahli, N. Noy, Selective cooperation between fatty acid binding proteins and peroxisome proliferator-activated receptors in regulating transcription, Mol. Cell. Biol. 22 (2002) 5114–5127.
[20] M. Saito, Y. Okamatsu-Ogura, M. Matsushita, K. Watanabe, T. Yoneshiro, J. Nio-Kobayashi, T. Iwanaga, M. Miyagawa, T. Kameya, K. Nakada, Y. Kawai, M. Tsujisaki, High incidence of metabolically active brown adipose tissue in healthy adult humans: effects of cold exposure and adiposity, Diabetes 58 (2009) 1526–1531.

Hypertension Research (2013) 36, 196–201

www.nature.com/hr

ORIGINAL ARTICLE

Cilnidipine regulates glucose metabolism and levels of high-molecular adiponectin in diet-induced obese mice

Daisuke Ueno, Takayuki Masaki, Koto Gotoh, Seiichi Chiba, Tetsuya Kakuma and Hironobu Yoshimatsu

The aim of the present study is to examine the effects of the antihypertensive drug cilnidipine on glucose metabolism and adipocytokines, including adiponectin, in diet-induced obese (DIO) mice. The effects of cilnidipine on insulin sensitivity and the levels of adiponectin in DIO mice were examined after the mice had been treated with cilnidipine dissolved in water at a dose of 0.2 g l^{-1} for 14 days. As expected, treatment with cilnidipine decreased the systolic and diastolic blood pressures in DIO mice, compared with control mice ($P<0.05$ for each parameter). Cilnidipine treatment improved glucose and insulin sensitivity in DIO mice. In addition, cilnidipine treatment dramatically increased the level of adiponectin in white adipose tissue ($P<0.05$) and the circulating levels of total and high-molecular weight (HMW) adiponectin in DIO mice ($P<0.01$ for each parameter). Furthermore, the secretion of HMW adiponectin and the ratio of HMW adiponectin/total adiponectin were both increased after cilnidipine treatment. Finally, the secretion of adiponectin from adipocytes was increased after cilnidipine treatment. Taken together, these results indicate that cilnidipine improves insulin tolerance and adiponectin levels, especially high-molecular type adiponectin, in DIO mice.
Hypertension Research (2013) 36, 196–201; doi:10.1038/hr.2012.141; published online 11 October 2012

Keywords: adiponectin; diabetes; obesity; white adipose tissue

INTRODUCTION

Several common disorders, such as hyperglycemia and hypertension, are seen in individuals with metabolic syndrome.[1] Metabolic disorders, such as diabetes and hypertension, are thought to be key to the simultaneous development of these common disorders in certain individuals, along with the associated development of cardiovascular and cerebrovascular disease.[2]

Previous studies demonstrated the presence of Ca^{2+} transport system and voltage-sensitive Ca^{2+} channels in adipocytes.[3] In addition, abnormal cellular calcium handling, particularly elevations in cytosolic-free calcium concentrations, are involved in insulin resistance and hypertension.[4] Antihypertensive drugs have been shown to have a therapeutic affect not only on blood pressure but also on other facets of metabolic disorders.[5,6] For instance, insulin sensitivity in patients with hypertension was improved after the administration of cilnidipine, a Ca channel blocker.[7] Thus, cilnidipine might be useful for patients with hypertension and diabetes mellitus based on its effects on glucose metabolism. However, the detailed mechanisms by which cilnidipine functions to ameliorate the effects of abnormal glucose metabolism remain unclear.

Several adipocytokines have crucial roles in the regulation of glucose metabolism.[8,9] Adipocytokines including tumor necrosis factor-alpha (TNF-alpha), IL-6 and resistin, which are all secreted from white adipose tissue (WAT), are known to be involved in glucose metabolism.[10–12] In addition, adiponectin and high-molecular weight (HMW) adiponectin have a number of vascular protective qualities, such as anti-diabetic, anti-inflammatory and anti-atherogenic effects.[13–16] Taken together, these findings suggest that adipocytokines regulate insulin sensitivity and may be related to the pathogenesis of diabetes.

In the present study, therefore, we focused on the effects of cilnidipine, an antihypertensive drug, on glucose metabolism and adipocytokine levels in diet-induced obesity. We hypothesized that cilnidipine might affect glucose metabolism as well as the production and/or secretion of adipocytokines. To address this issue, we used diet-induced obese (DIO) diabetic mice to investigate the effects of cilnidipine on metabolic parameters, such as glucose and insulin levels during a glucose/insulin tolerance test (ITT), and the levels of adipocytokines, such as TNF-alpha, IL-6, resistin and adiponectin, in WAT and serum.

METHODS

Animals

Mature male mice (C57Bl/6; Seac Yoshitomi, Fukuoka, Japan) were housed in a light-, temperature- and humidity-controlled room (12:12-h light:dark cycle, lights on/off at 0700 and 1900 hours, respectively; 21 ± 1 °C; 55 ± 5% relative humidity). The mice were allowed free access to 60% high-fat (HF) food (item D12492: 20% protein, 20% carbohydrate and 60% fat, 5.2 kcal g^{-1}; Research

Department of Internal medicine 1, Oita University, Oita, Japan
Correspondence: Dr T Masaki, Department of Internal medicine 1, Oita University, Oita 879-5593, Japan.
E-mail: masaki@oita-u.ac.jp
Received 5 January 2012; revised 27 July 2012; accepted 6 August 2012; published online 11 October 2012

Diet, Tokyo, Japan) and control diet (item D12450B: 3.9 kcal g^{-1}; Research Diet) and water. The HF food contained soybean oil (25/773.85 g) and lard (245/773.85 g). HF food was administered for 6 weeks, while the mice were between 8 and 14 weeks of age. All the animals were treated in accordance with the Oita University Guidelines for the Care and Use of Laboratory Animals.

Cilnidipine preparation and treatment

Cilnidipine (Mochida Pharmaceutical, Tokyo, Japan) and nicardipine (Sigma-Aldrich, Tokyo, Japan) were dissolved in vehicle (adjusted to pH 6.8–7.4). Each solution was prepared on the day that it was administered. We monitored drinking water of both the control and the cilnidipine treatment groups. Mice were selected and divided into two treatment groups. For the HF cilnidipine (*HF-CIL*) and HF nicardipine treatment groups, cilnidipine or nicardipine was added to the drinking water at a dose of 0.2 g l^{-1} for 14 consecutive days. The doses of cilnidipine and nicardipine were based on our preliminary data and a previous study.[17] As mentioned above, the control HF treatment group received untreated water for 14 consecutive days (last 2 weeks). The cumulative food intake was measured once every 24 h for each of the 14 days of treatment. Body weight, the histology of epididymal WAT, and the adipocytokine mRNA expression levels were examined and measured in all the animals at the end of the 14-day treatment period. WAT was dissected from the epididymal fat, mesenteric fat and retroperitoneal fat as visceral fat. The body fat mass was measured to assess changes in body fat accumulation in mice. The tissues were removed, weighed and immediately frozen in liquid nitrogen and then stored at −80 °C until subjected to mRNA extraction. The blood was withdrawn from the jugular vein, and the serum was separated and immediately frozen at −20 °C until assayed. The serum glucose, insulin, triglyceride and free fatty-acid levels were measured using commercially available assay kits (Wako Chemical, Tokyo, Japan).

Measurement of blood pressures

After treatment for 2 weeks, the systolic and diastolic blood pressures (SBP and DBP) and heart rate (HR) of the offspring were measured noninvasively using the tail-cuff method in conscious mice, as described previously (BP-2000; Visitech-Systems, Apex, NC, USA).[18]

Histological analysis

Epididymal WAT samples were fixed with 10% formalin and embedded in paraffin. Sections of 20 μm were cut and stained with hematoxylin and eosin to examine the histology of the white adipocytes used in the microscopy analysis system (Olympus, Tokyo, Japan).

Measurement of triglycerides in tissues

A total of 100 mg of epididymal WAT was homogenized using a polytron homogenizer (NS-310E; Micro Tech Nichion, Chiba, Japan) for 1 min in 2 ml of a solution containing NaCl at 1.5×10^{-4} mol l^{-1} (150 mM), 0.1% Triton X-100 and Tris at 1×10^{-3} mol l^{-1} (10 mM). The triglyceride content of this solution was determined using a commercially available kit (Wako Chemical).

Intraperitoneal glucose and ITT

After 4-h fasting, for the intraperitoneal glucose tolerance test or the ITT, the mice were treated with 2 g of glucose per kg body weight or 0.5 mU of regular insulin per g body weight via an intraperitoneal injection (Nobolin R; Novo Nordisk, Bagsvaerd, Denmark). Blood was sampled from the tail vein before and 30, 60 and 90 min after these injections, and the serum glucose and insulin concentrations were determined.

Cell culture and differentiation

Murine 3T3-L1 preadipocytes were obtained from the American Type Culture Collection (Dainippon Pharmaceutical, Osaka, Japan). Dulbecco's Modified Eagle Medium, fetal bovine serum, penicillin, streptomycin, D-biotin, insulin, dexamethasone and all other cell culture reagents were obtained from Wako Chemical. Cells were grown at 37 °C in 5% CO_2 in Dulbecco's Modified Eagle Medium containing 25 mM HEPES, 8 mg l^{-1} D-biotin, 100 U ml^{-1} penicillin and 10% fetal bovine serum (conditioned medium) and were seeded in six-well plates when used for experiments. Differentiation into mature adipocytes was induced by exposing the cells to conditioned medium supplemented with 1 μm of dexamethasone and 10 μg ml^{-1} of insulin (induction medium) for 2 days. Cells were then incubated with medium containing 5 μg ml^{-1} of insulin. After 2 days, the medium was replaced with the conditioned medium. Subsequently, the conditioned medium was changed regularly every 2 days. We have examined the effects of cilnidipine on adiponectin mRNA expression and secretion of adiponectin in 3T3-L1 adipocyte 12 h after CIL treatment. 3T3-L1 cells were pretreated with the concentration of cilnidipine (200 μm) for 12 h.

Real-time quantitative reverse transcription PCR

mRNAs were amplified using PCR and quantified using real-time quantitative PCR as follows. The total cellular RNA was prepared from selected mouse tissues using TRIzol (Lifetech, Tokyo, Japan) according to the manufacturer's protocol. Total RNA (20 μg) was electrophoresed on 1.2% formaldehyde-agarose gels. The RNA quality and quantity were assessed using ethidium bromide agarose gel electrophoresis and by calculating the 260:280 nm absorbance ratios. cDNA was synthesized from 150 ng of total RNA in a volume of 20 μl using a ReverTra-Dash reverse transcriptase kit (Toyobo, Tokyo, Japan) with random hexamer primers. Reactions were diluted to 50 μl with sterile distilled H_2O and stored at −20 °C. Primers were provided as qpre-optimized kits from Assay-on-Demand: resistin, IL-6 (the primers were generated by Nihon Gene Research Lab, Sendai, Japan), TNF-alpha (Mm00443258m1) and adiponectin (Mm00456425m1). Primers for ribosomal RNA, used as an internal control, were also provided as a pre-optimized kit (Hs99999901). PCR amplification was performed using an ABI PRISM 7000 sequence detector (Applied Biosystems, Foster City, CA, USA) in 50-μl volumes containing 100 ng of cDNA template in a PCR Master Mix (Roche, Nutley, NJ, USA) according to the following program: 50 °C for 2 min, 95 °C for 10 min, 40 cycles at 95 °C for 15 s and 60 °C for 1 min. Samples were analyzed in duplicate. The results were analyzed using Sequence Detection Software (Applied Biosystems), and the level of mRNA expression was normalized to that of ribosomal RNA as outlined in the Perkin-Elmer User Bulletin No. 2 (Perkin-Elmer, Wellesley, MA, USA).

Determination of levels of serum resistin, IL-6, TNF-alpha, and total and high-molecular weight adiponectin

The levels of WAT, serum resistin, IL-6, TNF-alpha, and total and HMW adiponectin were determined using an enzyme-linked immunosorbent assay kit (BioSource, Tokyo, Japan; Otsuka Pharmaceutical, Tokushima, Japan) and an optical density reader according to the manufacturer's instructions.

Statistical analysis

All data are expressed as the mean ± s.d. An unpaired *t*-test or analysis of variance *post-hoc* Bonferroni test was used to analyze statistical differences using StatView 4.0 (SAS Institute, Cary, NC, USA).

RESULTS

Effects of cilnidipine treatment on body weight, adiposity, glucose and insulin

Figure 1a summarizes the body weight and Figures 1b and c show the average food and drink intakes over the 6 weeks of the study period. No significant differences in the daily HF food consumption and body weight were noted between the cilnidipine-treated (HF-CIL) and the non-treated (HF) animals. Cilnidipine treatment, when compared with the results in the non-treated HF group, did not affect adiposity as assessed using the epididymal WAT weight (HF, 1.5 ± 0.2 g *vs.* HF-CIL, 1.6 ± 0.2 g, $P > 0.1$) or the mesenteric, retroperitoneal WAT weight and the triglyceride content of the epididymal WAT (Figures 1d–f, $P > 0.1$). We did not observe any notable morphological differences between the two groups (data not shown). In addition, both the serum glucose and insulin levels were not decreased in the HF-CIL group, compared with the untreated HF group (Figures 2a

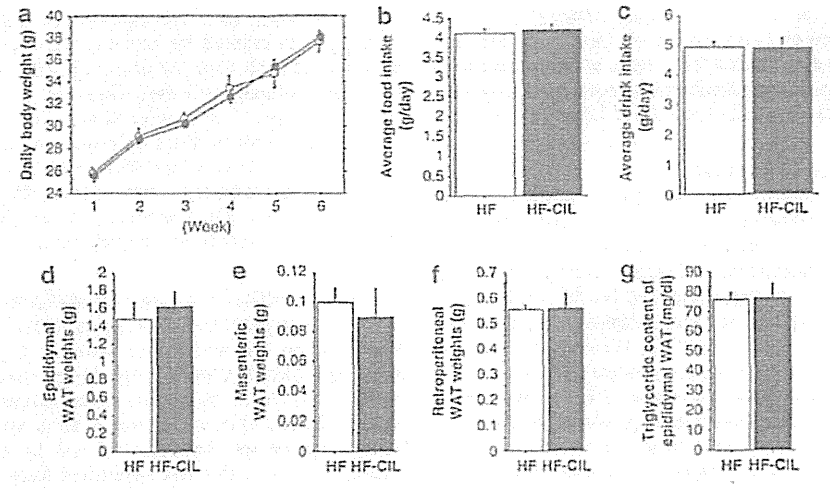

Figure 1 Effects of cilnidipine on (a) body weight changes (b) daily average food intake, (c) daily average drink intake, (d) weights of epididymal, (e) mesenteric and (f) retroperitoneal WAT and (g) triglyceride content of epididymal WAT in DIO mice. Results are shown for the control group not treated with cilnidipine (HF) and for the experimental group treated with cilnidipine (HF-CIL). Each value and vertical bar represents the mean ± s.d. ($n=4$ for each parameter).

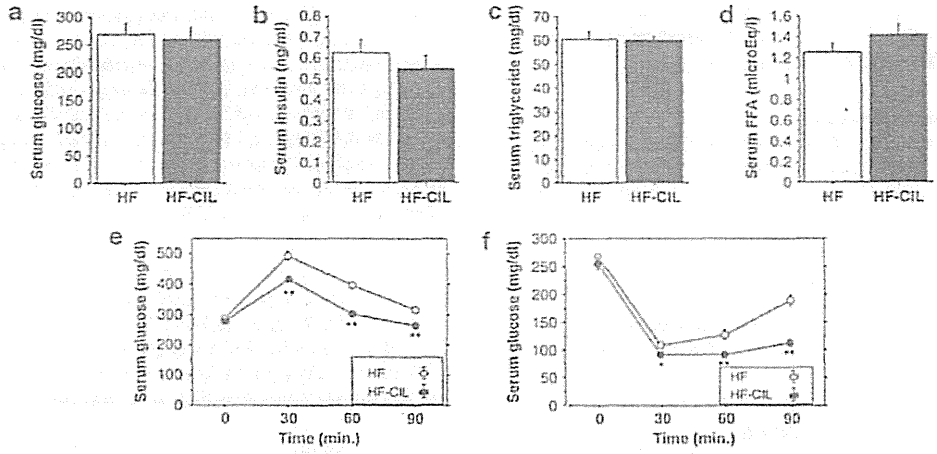

Figure 2 Effects of cilnidipine on (a) serum glucose, (b) serum insulin, (c) serum triglycerides, (d) serum free fatty acids and (e, f) glucose level changes during the intraperitoneal glucose and ITT in DIO mice. Results are shown for the HF and HF-CIL groups. Each value and vertical bar represents the mean ± s.d. (*$P<0.05$, **$P<0.01$ *vs.* control, $n=4$ for each parameter).

and b, $P>0.1$). The serum triglyceride and free fatty-acid levels were not significantly changed in the HF-CIL group (Figures 2c and d, $P>0.1$).

Effects of cilnidipine treatment on blood pressure and HR

The SBP and DBP were both higher in the DIO group, compared with the control groups ($P<0.01$). The SBP and DBP were not significantly changed before cilnidipine treatment (SBP: HF, 121 ± 4 mm Hg *vs.* HF-CIL, 122 ± 5 mm Hg; DBP: HF, 98 ± 3 mm Hg *vs.* HF-CIL, 99 ± 4 mm Hg, $P>0.1$ for each parameter). As expected, the SBP and DBP decreased with cilnidipine treatment (SBP: HF, 115 ± 3 mm Hg *vs.* HF-CIL, 98 ± 2 mm Hg; DBP: HF, 94 ± 3 mm Hg *vs.* HF-CIL, 84 ± 2 mm Hg, $P<0.01$ for each parameter). The HR tended to decrease, but the change was not significant compared with the controls (pre HR: HF, 605 ± 52 *vs.* HF-CIL, 627 ± 57; post HR: HF, 578 ± 65 *vs.* HF-CIL, 593 ± 72, $P>0.1$).

Intraperitoneal glucose and ITT

During the intraperitoneal glucose tolerance test, the CIL-treated mice showed lowered levels of blood glucose at each measurement point, compared with the controls (Figure 2e; $P<0.01$ for each parameter). The lowered glucose level in the CIL-treated mice persisted even 90 min after the initiation of the test. The levels of circulating insulin during the test were not significantly changed by CIL treatment. During the intraperitoneal ITT, the CIL-treated mice showed lowered levels of blood glucose at each measurement point, compared with the controls (Figure 2f; $P<0.05$ or <0.01 for each parameter).

Effects of nicardipine treatment on food intake body weight, glucose tolerance test and adiponectin levels

No significant differences in the daily HF food consumption and body weight were observed between the nicardipine-treated and the non-treated animals (Figures 3a and b). The SBP and DBP decreased significantly with nicardipine treatment (SBP: HF, 120 ± 3 mm Hg *vs.* HF nicardipine, 104 ± 2 mm Hg; DBP: HF, 96 ± 3 mm Hg *vs.* HF nicardipine, 87 ± 1 mm Hg, $P<0.01$ for each parameter). The improvements of glucose metabolism during the intraperitoneal glucose tolerance test were not observed in mice treated with nicardipine (Figure 3c). In addition, the levels of HMW and total adiponectin in the sera were not significantly changed by nicardipine treatment (Figure 3d).

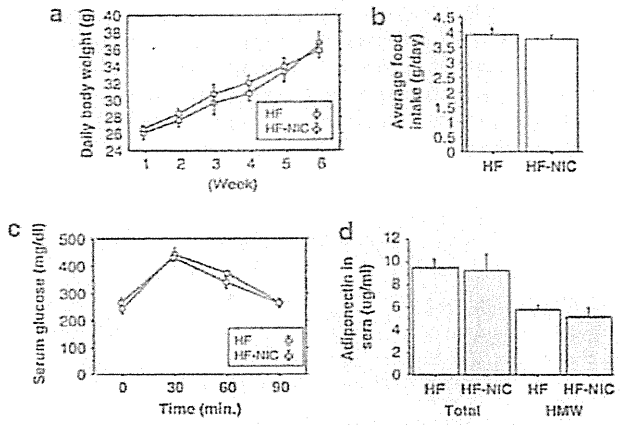

Figure 3 Effects of nicardipine on (a) body weight changes (b) daily average food intake, (c) glucose levels during the intraperitoneal glucose tolerance test and (d) serum total and HMW adiponectin levels in DIO mice. Results are shown for the control group not treated with nicardipine (HF) and for the experimental group treated with nicardipine (HF nicardipine). Each value and vertical bar represents the mean ± s.d. ($n=4$ for each parameter).

Effects of cilnidipine treatment on inflammatory adipocytokine levels

We examined the mRNA expression and serum levels of TNF-alpha, resistin and IL-6 in epididymal WAT and found that none of these levels (Figures 4a–c) were altered in the HF-CIL group, compared with the HF group (TNF-alpha mRNA: HF, 100 ± 14% *vs.* HF-CIL, 98 ± 25%; resistin mRNA: HF, 100 ± 20% *vs.* HF-CIL, 113 ± 32%; IL-6 mRNA: HF, 100 ± 14% *vs.* HF-CIL, 88 ± 23%, $P>0.1$ for each parameter).

Effect of cilnidipine treatment on adiponectin level

Figure 4d shows that the adiponectin mRNA levels in epididymal and retroperitoneal WAT were increased in the HF-CIL group, compared with the HF group (epididymal WAT: HF, 100 ± 16% *vs.* HF-CIL, 178 ± 26%, $P<0.05$; mesenteric WAT: HF, 100 ± 12% *vs.* HF-CIL, 111 ± 15%, $P>0.1$; retroperitoneal WAT: HF, 100 ± 16% *vs.* HF-CIL, 162 ± 34%, $P<0.05$). Similarly, Figure 4e shows that the serum levels of total adiponectin and HMW adiponectin were both significantly increased in the HF-CIL group, compared with the control HF group ($P<0.05$ or <0.01). Of note, the ratio of HMW/total adiponectin in the sera increased dramatically with CIL treatment (Figure 4f).

Effect of cilnidipine treatment on total and HMW adiponectin levels in adipocytes

Figures 5a and b show the levels of adiponectin in 3T3-L1 cells after cilnidipine treatment. The mRNA expression level of adiponectin in the 3T3-L1 cells was increased in the CIL group, compared with the CONT group ($P<0.05$). Similarly, the level of adiponectin in the medium was increased in the 3T3-L1 cells (CONT, 2.4 ± 0.2 μg ml^{-1} *vs.* CIL, 3.5 ± 0.2 μg ml^{-1}, $P<0.05$). There was no significantly change in the levels of TNF-alpha and INF-gamma between the groups (TNF-alpha: CONT, 4.1 ± 1.3 pg ml^{-1} *vs.* CIL, 5.1 ± 0.9 pg ml^{-1}, $P>0.1$; INF-gamma: CONT, 2.3 ± 0.5 pg ml^{-1} *vs.* CIL, 2.6 ± 0.4 pg ml^{-1}, $P>0.1$).

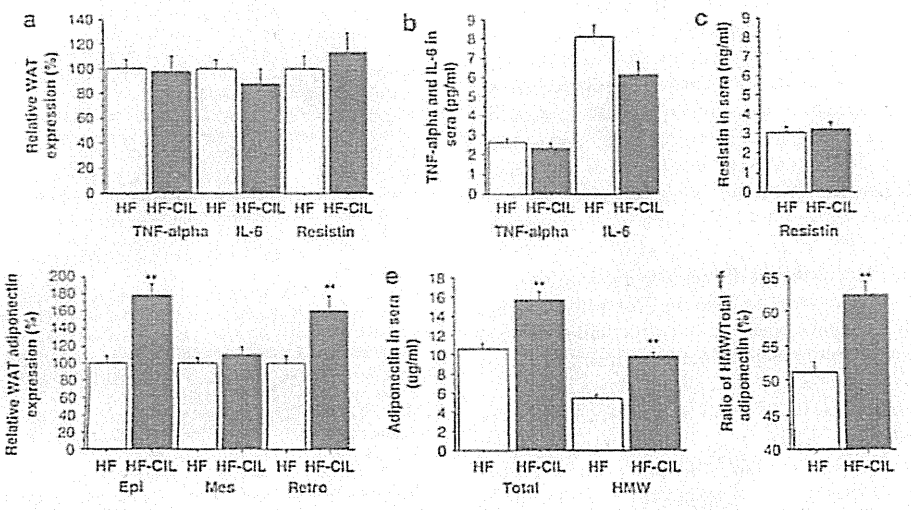

Figure 4 Effects of cilnidipine on (a) TNF-alpha mRNA, IL-6 mRNA and resistin mRNA expression levels in epididymal WAT, and (b) circulating TNF-alpha, IL-6, (c) circulating resistin, (d) adiponectin mRNA expression levels in WAT, (e) serum adiponectin levels and (f) the ratio of serum HMW/total adiponectin in DIO mice. Results are shown for the HF-CIL and HF groups. Each value and vertical bar represents the mean ± s.d. (*$P<0.05$, **$P<0.01$ *vs.* control, $n=4$ for each parameter).

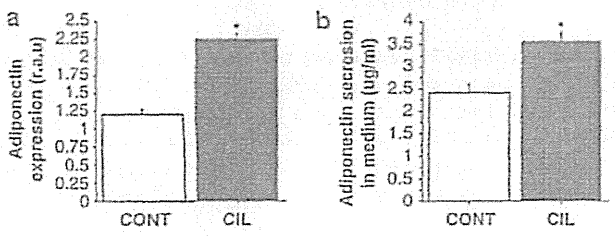

Figure 5 Effects of cilnidipine on (a) adiponectin mRNA expression and (b) secretion of adiponectin in 3T3-L1 adipocyte 12 h after CIL treatment at a dose of 200 μm. Results are shown for the HF-CIL and HF groups. Each value and vertical bar represents the mean ± s.d. (*$P<0.05$ vs. control, $n=4$ for each parameter).

DISCUSSION

In the present study, we have demonstrated that the calcium channel inhibitor cilnidipine improves glucose and insulin tolerance accompanied by an increase in adiponectin in DIO mice. Obesity and/or fat accumulation are well known to lead potentially to insulin resistance, although a reduction in body weight or adiposity can minimize problems, such as insulin resistance, that are often associated with obesity-related metabolic disorders.[19] In the present study, however, cilnidipine treatment did not affect either the body weight or adiposity. Therefore, cilnidipine treatment may modify glucose metabolism and/or insulin sensitivity independent of body adiposity.

The pharmacological properties of cilnidipine, which acts as an L-type and an N-type calcium channel antagonist, should be mentioned.[7,20] L-type and/or N-type calcium channel drugs are known to affect insulin resistance favorably,[7,20] and the regulation of sympathetic nerves may affect insulin signaling, thereby affecting the activity of intracellular signaling molecules including adipocytes.[21–23] In addition to signaling molecules in adipocytes, a number of factors have been shown to be involved in regulating insulin resistance by adipocytokines, such as adiponectin and TNF-alpha.[8–11] In the present study, we focused on the effect of cilnidipine on the adipocytokines resistin, IL-6, TNF-alpha and adiponectin. Treatment with cilnidipine did not affect the levels of resistin, IL-6 or TNF-alpha in serum or WAT. However, we found that cilnidipine treatment regulated the levels of adiponectin in WAT and sera. Adiponectin is known to be an insulin-sensitizing adipocytokine[24] that regulates glucose metabolism by accelerating insulin signaling and glucose uptake in the liver and skeletal muscles.[25] Adiponectin also regulates markers of inflammation, contributing to its positive effect on insulin sensitivity.[26,27] These findings suggested that adiponectin might be involved in cilnidipine-induced improvements in insulin sensitivity in DIO mice. In the present study, L-type calcium channel antagonist nicardipine did not significantly influence the glucose metabolism and adiponectin levels in DIO mice. Although the detailed mechanisms remain unknown, N-type calcium channels may effectively influence adiponectin and/or cilnidipine may have pleiotropic effects on adiponectin.

Adiponectin is generally present in serum as a trimer, hexamer or HMW form.[27] Among the forms of adiponectin, the HMW adiponectin form is the most active and confers a protective effect on blood vessels.[28] Furthermore, HMW adiponectin appears to be better associated with insulin sensitivity than total adiponectin and to be strongly associated with a lower risk for incident diabetes,[29] coronary artery disease[30] and cerebrovascular disease. Interestingly, cilnidipine treatment accelerated the secretion of HMW adiponectin. This result suggests that cilnidipine may improve glucose metabolism in a manner involving HMW adiponectin. The present study provides novel insights into the involvement of cilnidipine as a therapeutic tool in the treatment of metabolic syndrome, including hypertension and insulin resistance. Several studies presented the nifedipine influenced on glucose metabolism, lipid oxidation and adipocyte dysfunction.[31,32] Thus, it is possible that several calcium channel blockers, including cilnidipine, have an action on adipocyte.

The present study has several limitations. First, this study is pharmacologically experiment and the dose of cilnidipine in this study is relatively high. Second, the number of mice might not be enough. Third, the experiments using specific inhibitor of N-type Ca channel or deficient mice of the channel would be useful. Further basic and clinical studies are needed to clarify the detail mechanisms of cilnidipine.

In summary, the results of our study suggest that cilnidipine treatment may prevent the development of insulin resistance without affecting body adiposity in DIO mice. Associated changes in the levels and/or activity of adiponectin, especially HMW adiponectin, may contribute to the beneficial therapeutic effect of cilnidipine on metabolic disorders.

CONFLICT OF INTEREST

The authors declare no conflict of interest.

ACKNOWLEDGEMENTS

This work was supported by a grant from the Japanese Ministry of Education, Science and Culture and Research on Measures for Intractable Diseases, Japanese Ministry of Health, Welfare and Labor, Japan.

1 Kong AP, Chan NN, Chan JC. The role of adipocytokines and neurohormonal dysregulation in metabolic syndrome. *Curr Diabetes Rev* 2006; 2: 397–407.
2 Mottillo S, Filion KB, Genest J, Joseph L, Pilote L, Poirier P, Rinfret S, Schiffrin EL, Eisenberg MJ. The metabolic syndrome and cardiovascular risk a systematic review and meta-analysis. *J Am Coll Cardiol* 2010; 56: 1113–1132.
3 Pershadsingh HA, Lee LY, Snowdowne KW. Evidence for a sodium/calcium exchanger and voltage-dependent calcium channels in adipocytes. *FEBS Lett* 1989; 244: 89–92.
4 Nanberg E, Connolly E, Nedergaard J. Presence of a Ca2 + -dependent K + channel in brown adipocytes. Possible role in maintenance of alpha 1-adrenergic stimulation. *Biochim Biophys Acta* 1985; 844: 42–49.
5 Araki K, Masaki T, Katsuragi I, Tanaka K, Kakuma T, Yoshimatsu H. Telmisartan prevents obesity and increases the expression of uncoupling protein 1 in diet-induced obese mice. *Hypertension* 2006; 48: 51–57.
6 Sugimoto K, Qi NR, Kazdova L, Pravenec M, Ogihara T, Kurtz TW. Telmisartan but not valsartan increases caloric expenditure and protects against weight gain and hepatic steatosis. *Hypertension* 2006; 47: 1003–1009.
7 Yagi S, Goto S, Yamamoto T, Kurihara S, Katayama S. Effect of cilnidipine on insulin sensitivity in patients with essential hypertension. *Hypertens Res* 2003; 26: 383–387.
8 Matsuzawa Y. The metabolic syndrome and adipocytokines. *FEBS Lett* 2006; 580: 2917–2921.
9 Kadowaki T, Yamauchi T. Adiponectin and adiponectin receptors. *Endocr Rev* 2005; 26: 439–451.
10 Dandona P, Aljada A, Bandyopadhyay A. Inflammation: the link between insulin resistance, obesity and diabetes. *Trends Immunol* 2004; 25: 4–7.
11 Uysal KT, Wiesbrock SM, Marino MW, Hotamisligil GS. Protection from obesity-induced insulin resistance in mice lacking TNF-alpha function. *Nature* 1997; 389: 1997.
12 Galic S, Oakhill JS, Steinberg GR. Adipose tissue as an endocrine organ. *Mol Cell Endocrinol* 2010; 316: 129–139.
13 Masaki T, Chiba S, Tatsukawa H, Yasuda T, Noguchi H, Seike M, Yoshimatsu H. Adiponectin protects LPS-induced liver injury through modulation of TNF-alpha in KK-Ay obese mice. *Hepatology* 2004; 40: 177–184.
14 Masaki T, Chiba S, Yasuda T, Tsubone T, Kakuma T, Shimomura I, Funahashi T, Matsuzawa Y, Yoshimatsu H. Peripheral, but not central, administration of adiponectin reduces visceral adiposity and upregulates the expression of uncoupling protein in agouti yellow (Ay/a) obese mice. *Diabetes* 2003; 52: 2266–2273.
15 Shimada K, Miyazaki T, Daida H. Adiponectin and atherosclerotic disease. *Clin Chem Acta* 2004; 344: 1–12.
16 Hotta K, Funahashi T, Bodkin NL, Ortmeyer HK, Arita Y, Hansen BC, Matsuzawa Y. Circulating concentrations of the adipocyte protein adiponectin are decreased in

parallel with reduced insulin sensitivity during the progression to type 2 diabetes in rhesus monkeys. *Diabetes* 2001; 50: 1126–1133.
17 Fan YY, Kohno M, Nakano D, Ohseki H, Kobori H, Suwami D, Ohashi N, Hitomi H, Asanuma K, Noma T, Tomino Y, Fujita T, Nishiyama A. Cilnidipine suppresses podocyte injury and proteinuria in metabolic syndrome rats: possible involvement of N-type calcium channel in podocyte. *J Hypertens* 2010; 28: 1034–1043.
18 Yano M, Yamamoto Y, Yoshida M, Ueda S, Latifpour J. Effects of doxazosin on blood flow and mRNA expression of nitric oxide synthase in the spontaneously hypertensive rat genitourinary tract. *Life Sci* 2007; 8: 218–222.
19 Jacob S, Machann J, Rett K, Brechtel K, Volk A, Renn W, Maerker E, Matthaei S, Schick F, Claussen CD, Haring HU. Association of increased intramyocellular lipid content with insulin resistance in lean nondiabetic offspring of type 2 diabetic subjects. *Diabetes* 1999; 48: 1113–1119.
20 Masuda T, Ogura MN, Moriya T, Takahira N, Matsumoto T, Kutsuna T, Hara M, Aiba N, Noda C, Izumi T. Beneficial effects of L- and N-type calcium channel blocker on glucose and lipid metabolism and renal function in patients with hypertension and type II diabetes mellitus. *Cardiovasc Ther* 2011; 29: 46–53.
21 Thorens B. Glucose sensing and the pathogenesis of obesity and type 2 diabetes. *Int J Obes (Lond)* 2008; 32: S62–S71.
22 McCarty MF. Elevated sympathetic activity may promote insulin resistance syndrome by activating alpha-1 adrenergic receptors on adipocytes. *Med Hypotheses* 2004; 62: 830–838.
23 Mulder AH, Tack CJ, Olthaar AJ, Smits P, Sweep FC, Bosch RR. A drenergic receptor stimulation attenuates insulin-stimulated glucose uptake in 3T3-L1 adipocytes by inhibiting GLUT4 translocation. *Am J Physiol Endocrinol Metab* 2005; 289: E627–E633.
24 Stefan N, Vozarova B, Funahashi T, Matsuzawa Y, Weyer C, Lindsay RS, Youngren JF, Havel PJ, Pratley RE, Bogardus C, Tataranni PA. Plasma adiponectin concentration is associated with skeletal muscle insulin receptor tyrosine phosphorylation, and low plasma concentration precedes a decrease in whole-body insulin sensitivity in humans. *Diabetes* 2002; 50: 1884–1888.
25 Yamauchi T, Kamon J, Minokoshi Y, Ito Y, Waki H, Uchida S, Yamashita S, Noda M, Kita S, Ueki K, Eto K, Akanuma Y, Froguel P, Foufelle F, Ferre P, Carling D, Kimura S, Nagai R, Kahn BB, Kadowaki T. Adiponectin stimulates glucose utilization and fatty-acid oxidation by activating AMP-activated protein kinase. *Nat Med* 2002; 8: 1288–1295.
26 Shetty S, Kusminski CM, Scherer PE. Adiponectin in health and disease: evaluation of adiponectin-targeted drug development strategies. *Trends Pharmacol Sci* 2009; 30: 234–239.
27 Hirose H, Yamamoto Y, Seino-Yoshihara Y, Kawabe H, Saito I. Serum high-molecular-weight adiponectin as a marker for the evaluation and care of subjects with metabolic syndrome and related disorders. *J Atheroscler Thromb* 2010; 17: 1201–1211.
28 Kobayashi H, Ouchi N, Kihara S, Walsh K, Kumada M, Abe Y, Funahashi T, Matsuzawa Y. Selective suppression of endothelial cell apoptosis by the high molecular weight form of adiponectin. *Circ Res* 2004; 94: e27–e31.
29 Nakashima R, Kamei N, Yamane K, Nakanishi S, Nakashima A, Kohno N. Decreased total and high molecular weight adiponectin are independent risk factors for the development of type 2 diabetes in Japanese-Americans. *J Clin Endocrinol Metab* 2006; 91: 3873–3877.
30 von Eynatten M, Humpert PM, Bluemm A, Lepper PM, Hamann A, Allolio B, Nawroth PP, Bierhaus A, Dugi KA. High-molecular weight adiponectinis independently associated with extent of coronary artery disease in men. *Atherosclerosis* 2008; 199: 123–128.
31 Iwai M, Kanno H, Inaba S, Senba I, Sone H, Nakaoka H, Nifedipine Horiuchi M. A calcium-channel blocker, attenuated glucose intolerance and white adipose tissue dysfunction in type 2 diabetic KK-A(y) mice. *Am J Hypertens* 2011; 24: 169–174.
32 Tian Z, Miyata K, Tabata M, Yano M, Tazuma H, Aoi J, Takahashi O, Araki K, Kawasuji M, Oike Y. Nifedipine increases energy expenditure by increasing PGC-1α expression in skeletal muscle. *Hypertens Res* 2011; 34: 1221–1227.

Journal of Neurochemistry JNC

JOURNAL OF NEUROCHEMISTRY | 2013 | 124 | 90–99 doi: 10.1111/jnc.12066

ORIGINAL ARTICLE

Nesfatin-1, corticotropin-releasing hormone, thyrotropin-releasing hormone, and neuronal histamine interact in the hypothalamus to regulate feeding behavior

Koro Gotoh, Takayuki Masaki, Seiichi Chiba, Hisae Ando, Takanobu Shimasaki, Kimihiko Mitsutomi, Kansuke Fujiwara, Isao Katsuragi, Tetsuya Kakuma, Toshiie Sakata and Hironobu Yoshimatsu

Department of Internal Medicine 1, Faculty of Medicine, Oita University, Yufu, Japan

Abstract

Nesfatin-1, corticotropin-releasing hormone (CRH), thyrotropin-releasing hormone (TRH), and hypothalamic neuronal histamine act as anorexigenics in the hypothalamus. We examined interactions among nesfatin-1, CRH, TRH, and histamine in the regulation of feeding behavior in rodents. We investigated whether the anorectic effect of nesfatin-1, α-fluoromethyl histidine (FMH; a specific suicide inhibitor of histidine decarboxylase that depletes hypothalamic neuronal histamine), a CRH antagonist, or anti-TRH antibody affects the anorectic effect of nesfatin-1, whether nesfatin-1 increases CRH and TRH contents and histamine turnover in the hypothalamus, and whether histamine increases nesfatin-1 content in the hypothalamus. We also investigated whether nesfatin-1 decreases food intake in mice with targeted disruption of the histamine H1 receptor (H1KO mice) and if the H1 receptor (H1-R) co-localizes in nesfatin-1 neurons. Nesfatin-1-suppressed feeding was partially attenuated in rats administered with FMH, a CRH antagonist, or anti-TRH antibody, and in H1KO mice. Nesfatin-1 increased CRH and TRH levels and histamine turnover, whereas histamine increased nesfatin-1 in the hypothalamus. Immunohistochemical analysis revealed H1-R expression on nesfatin-1 neurons in the paraventricular nucleus of the hypothalamus. These results indicate that CRH, TRH, and hypothalamic neuronal histamine mediate the suppressive effects of nesfatin-1 on feeding behavior.

Keywords: CRH, feeding behavior, histamine, hypothalamus, nesfatin-1, TRH.

J. Neurochem. (2013) **124**, 90–99.

The gene encoding nucleobindin-2 (NUCB2) in the hypothalamus can be cleaved into the novel peptides, nesfatin-1, -2, and -3 (Oh-I *et al.* 2006). Nesfatin-1, but neither nesfatin-2 nor nesfatin-3, reduces dark-phase food intake in rats when injected into the third ventricle (Oh-I *et al.* 2006). Although a nesfatin-1 receptor has not been identified, several studies have demonstrated abundant NUCB2/nesfatin-1 expression in the hypothalamic and medullary sites involved in feeding regulation in rats, including the paraventricular nucleus (PVN), the arcuate nucleus (ARC), and the nucleus of the solitary tract (NTS) (Brailoiu *et al.* 2007; Berthoud and Morrison 2008; Elmquist *et al.* 2009; Goebel *et al.* 2009). These findings support the notion that nesfatin-1 is involved in the regulation of food intake. Levels of NUCB2 mRNA and nesfatin-1 are significantly decreased in the PVN of rats deprived of food for 24 h compared with that of rats fed *ad libitum*, suggesting that nesfatin-1 in the PVN plays a role in satiety, and possibly energy homeostasis, after food intake (Oh-I *et al.* 2006). Conversely, daily food consumption increased and body weight cumulatively increased after endogenous NUCB2 was blocked by administering an anti-NUCB2 antisense oligonucleotide into the third ventricle (Oh-I *et al.* 2006).

Received June 23, 2012; revised manuscript received October 16, 2012; accepted October 17, 2012.

Address correspondence and reprint requests to Koro Gotoh, Department of Internal Medicine 1, Faculty of Medicine, Oita University, Yufu, Oita 879-5593, Japan. E-mail: gotokoro@oita-u.ac.jp

Abbreviations used: ARC, arcuate nucleus; BBB, blood–brain barrier; CRH, corticotropin-releasing hormone; FMH, α-fluoromethyl histidine; HDC, histidine decarboxylase; MCH, melanin-concentrating hormone; NUCB2, nucleobindin-2; PBS, phosphate-buffered saline; PVN, paraventricular nucleus; TMN, tuberomammillary nucleus; TRH, thyrotropin-releasing hormone; VMH, ventromedial nucleus.

Hypothalamic histamine neurons originating from the tuberomammillary nucleus (TMN) distributed in the posterior hypothalamus project diffusely throughout the brain, including the PVN and the ventromedial nucleus (VMH), which is known as the satiety center (Kennedy 1950). Other study showed that hypothalamic histamine suppresses food intake via histamine H1-receptor (H1-R) in VMH and PVN (Fukagawa *et al.* 1989), several distinct endogenous peptides in the PVN such as corticotropin-releasing hormone (CRH) and thyrotropin-releasing hormone (TRH), inhibit food intake (Kow and Pfaff 1991; Richard *et al.* 2000). Moreover, CRH and TRH directly activate histamine neurons (Gotoh *et al.* 2005, 2007). Based on these findings, we hypothesized that nesfatin-1, CRH, TRH, and hypothalamic neuronal histamine constitute a neuronal network within the hypothalamus that regulates energy metabolism. The aim of this study was to examine whether nesfatin-1 affects the expressions of CRH or TRH and histamine turnover in the hypothalamus, whether a central infusion of histamine activates nesfatin-1 neurons and whether nesfatin-1 expression is altered in H1KO mice.

Methods

Animals

Male Sprague-Dawley rats weighting 250–280 g (Seac Yoshitomi, Fukuoka, Japan), male C57BL/6N mice weighting 25–30 g (Seac Yoshitomi), and male H1KO mice weighting 25–30 g (Kyushu University, Fukuoka, Japan) were used. They were housed in a room with daily illumination from 07:00 to 19:00 (12/12-h light/dark cycle) and maintained at 21 ± 1°C with 55 ± 5% humidity. H1-R knockout (H1KO) mice that lack the H1-R neuronal histamine receptor for backcrossing were maintained at Oita University (Yufu, Japan). Backcrossing H1-R−/− homozygous mice with the C57BL/6N strain (Kyudo, Fukuoka, Japan) for six generations resulted in incipient congenital N5 mice with two genotypes (H1-R−/− and H1-R+/+). All genotypes were confirmed by Southern blotting as described (Inoue *et al.* 1996). Animals were fed standard chow (Clea chow, Clea, Japan), allowed access to and tap water *ad libitum*, and handled for 5 min each on four successive days to habituate arousal levels before the experiment. On test days, all animals had recovered to at least their pre-experiment body weight. All experiments proceeded in accordance with the Oita University Guidelines, which are based on the Guide for the Care and Use of Laboratory Animals published by the National Institutes of Health.

Surgery

Rats were placed in a stereotaxic apparatus under intraperitoneal (i.p.) anesthesia with 100 mg/kg of sodium pentobarbital (Narishige, Tokyo, Japan). The implantation of a chronic cannula (a 23-gauge stainless steel; length, 15 mm) into the third cerebroventricle (3vt) was performed at least 10 days before starting infusions. A 30-gauge stainless steel wire stylet was inserted into the guide cannula to prevent cerebrospinal fluid (CSF) leakage and cannula obstruction. A chronic cannula was inserted into the 3vt along the midline, 6.0-mm anterior to the zero ear bar coordinate, to a depth of 7.8 mm from the cortical surface according to the atlas of Paxinos and Watson (1986).

At least 1 week before starting infusions, a cannula was similarly implanted into the lateral cerebroventricle (lvt) of the mice, 1.0-mm lateral to the midline, and 0.22-mm posterior to the bregma at a depth of 2.0 mm from the cortical surface, according to the atlas of Franklin and Paxinos (1997).

Reagents

On the day of the experiment, L-histamine (0.1 μmol/μL), recombinant nesfatin-1 (5 ng/μL; Sigma Chemical Co., St Louis, MO, USA), α-helical $CRH_{9\text{-}41}$ (α-helical CRH, 1 μg/μL; Sigma) which is a competitive CRH receptor antagonist that blocks both CRH types 1 (CRH1-R) and 2 (CRH2-R) receptors, rabbit anti-TRH serum that neutralizes endogenous TRH of rat (Antibodies-online GmbH, Atlanta, GA, USA), pargyline hydrochloride (1 mmol/mL), and α-fluoromethylhistidine (FMH), a suicide inhibitor of histidine decarboxylase (HDC) (100 μg/μL; Research Biochemical International, Natick, MA, USA) were dissolved in a fresh phosphate-buffered saline (PBS) and the pH was adjusted to 6.5–7.5.

Experimental protocol

Experiment 1: A total of 108 rats were divided into 18 groups (n = 6 per group) as follows: the PBS/PBS (4 groups, n = 6 in each), FMH/PBS (2 groups, n = 6 in each), PBS/nesfatin-1(3vt, 3 groups, n = 6 in each), PBS/nesfatin-1(i.p.), FMH/nesfatin-1(3vt), FMH/nesfatin-1(i.p.), α-helical CRH (10 or 50 μg)/PBS (n = 6 in each), α-helical CRH (50 μg)/nesfatin-1(3vt), anti-TRH serum/PBS, and anti-TRH serum/nesfatin-1(3vt) groups. They were pre-treated with an 3vt injection of FMH (1 mg/10 μL/10 min; this dose depletes most neuronal histamine in the hypothalamus), α-helical CRH (10 or 50 μg/10 μL/10 min), anti-TRH serum (10 μL/10 min, this dose decreases rectal temperature by approximately 1°C; Prasad *et al.* 1980) or PBS (10 μL/10 min) at 2 h before a further 3vt or i.p. injection of nesfatin-1 (30 ng/10 μL/10 min), or 3vt infusion of PBS (10 μL/10 min).

Experiment 2: Twelve wild-type and 12 H1KO mice were divided into the nesfatin-1 (5 ng/1 μL/1 min; lvt) and PBS (1 μL/1 min; lvt) groups, respectively (n = 6 in each).

Measurement of food intake in rats and mice

Food intake was measured in rats and mice fed ad libitum for 4 h during the dark phase (between 19:00 and 23:00 h) after the administration of each agent as described above, using an indirect calorimetry system (Columbus Instruments, Columbus, OH, USA).

CRH, TRH, and tele-methylhistamine contents, and histamine-regulated changes in hypothalamic and plasma nesfatin-1 levels

Forty-two rats were divided into seven equal groups (n = 6 per group) as follows: the PBS/PBS, α-helical CRH/PBS, anti-TRH serum/PBS, PBS/nesfatin-1(3vt), PBS/nesfatin-1(i.p.), α-helical CRH/nesfatin-1 (50 ng, 3vt), and anti-TRH serum/nesfatin-1(3vt) and PBS/histamine (1 μmol/10 μL/10 min) groups. Each group was pre-treated by i.p. administration of pargyline hydrochloride (0.33 mmol/kg), which inhibits monoamine oxidase B and induces the extraneuronal accumulation of tele-methylhistamine (t-MH), a

major metabolite of released neuronal histamine. All rats were anesthetized with sodium pentobarbital (100 mg/kg, i.p.), and then given a transcardiac perfusion of 100 mL of saline containing 200 U heparin. Each rat was decapitated, and then sections containing the hypothalamus were cut according to the rat brain atlas of Paxinos and Watson (1986) to measure t-MH content. Tissue blocks were homogenized in 400 μL of 0.5 M acetic acid, boiled for 10 min, and then protein was assayed (Bio-Rad, Hercules, CA, USA) in 50 μL aliquots. Blood from all rats obtained by cardiac puncture was collected into tubes containing EDTA (7.5%, 10 μL/0.5 mL blood; Sigma Chemical Co.) and aprotinin (0.6 U trypsin inhibitor/0.5 mL blood; ICN Pharmaceuticals, Costa Mesa, CA, USA) and then separated by centrifugation at 4000 *g* for 10 min at 4°C. Plasma was immediately frozen and stored at −80°C. The CRH and TRH contents were measured in PVN-specific hypothalamus section punches dissected with a frozen blade, using CRH (Yanaihara Co. Shizuoka, Japan) and a TRH (Life Science Inc., Houston, TX, USA) ELISA kits. Plasma and hypothalamic nesfatin-1 levels were measured in punches from LH-, PVN-, VMH-, and TMN-specific sections using a nesfatin-1 EIA kit (Phoenix Pharmaceuticals Inc., Burlingame, CA, USA). The t-MH content in the LH, PVN, VMH, and TMN was assayed by HPLC using deproteinized supernatants containing amine extracts. Details of the amine assays are described elsewhere (Sakata *et al.* 1981).

Immunohistochemistry

Rats were anesthetized using 100 mg/kg sodium pentobarbital i.p., and killed by transcardiac perfusion with 50 mL PBS that contained 50 U heparin, followed by 50 mL 4% *p*-formaldehyde in PBS. The brains were removed and divided into forebrain, diencephalon, and brainstem segments. The specimens were rapidly frozen at −80°C and sectioned at a thickness of 40 μm using a cryostat at −20°C. The sections were incubated overnight at 4°C with polyclonal rabbit antiserum against rat HDC (1 : 2000; Chemicon Inc., Temecula, CA, USA), followed by biotin-conjugated goat anti-rabbit IgG and fluorescein isothiocyanate-conjugated streptavidin (ABC reagent; Vector Laboratories, Burlingame, CA, USA). Next, they were incubated with a specific polyclonal rabbit antiserum against rat nesfatin-1 (1 : 2000; Phoenix Pharmaceuticals Inc.) in 0.3% Triton X-100 containing 1% normal rabbit serum. Biotin-conjugated secondary IgG antibodies (ABC reagent; Vector Laboratories) were added, followed by rhodamine-conjugated streptavidin (ABC reagent; Vector Laboratories).

Other sections were incubated overnight at 4°C with a specific polyclonal rabbit antiserum against rat nesfatin-1 (1 : 2000; Phoenix Pharmaceuticals Inc.) and a specific polyclonal rabbit antiserum against rat H1-R (1 : 1000; Millipore, Billerica, MA, USA). The sections were then incubated with biotin-conjugated secondary IgG antibody (ABC reagent; Vector Laboratories), fluorescein isothiocyanate-conjugated streptavidin for H1-R and rhodamine-conjugated streptavidin (ABC reagent; Vector Laboratories) for nesfatin-1. The negative controls in each experiment were incubated with normal serum instead of the primary antibody (nesfatin-1 or H1-R), followed by both secondary antibodies. We determined the specificity of the nesfatin-1 and H1-R antisera, after incubating each with recombinant nesfatin-1 (Sigma) or H1-R (Gene Tex Inc., Irvine, CA, USA) protein. Increasing amounts of protein were added to a fixed concentration of nesfatin-1 and H1-R antiserum at a 1 : 1, 1 : 5, and 1 : 10 molar ratio to the concentration of each recombinant protein. Stained sections were analyzed using a confocal immunofluorescence microscope (Olympus, Tokyo, Japan) and imaging software (Lumina Vision; Mitsutani Corp., Tokyo, Japan). The resultant digital images of the same section were not adjusted or altered, except for an occasional change in brightness. Nesfatin-1 or H1-R immunoreactivity was determined by drawing areas of PVN in hypothalami and applying an optical density scale using automated counting tools from the imaging software (Lumina Vision; Mitsutani Corp.). Ratios of co-expressed signals were also assessed by counting single-labeled nesfatin-1 and double-labeled nesfatin-1 and H1 receptor-positive neurons. Every fifth section of serial hypothalamus samples from six rats (seven sections per rat) was analyzed.

Western blotting

We examined the molecular weight of proteins recognized by the nesfatin-1 and H1-R antibodies by western blotting recombinant nesfatin-1 (Sigma), and H1-R (Gene Tex Inc.) protein in the hypothalamus of rats. These proteins were diluted to final concentrations in sample buffer (50 mM Tris-HCl, pH 8.0, 10% glycerol, 1 mM EDTA, 2 mM dithiothreitol, and 1 mM *o*-vanadate), heated at 94°C for 4 min, and then separated by centrifugation (12 000 *g*) for 5 min. The supernatants were resolved by 7.5% sodium dodecyl sulfate–polyacrylamide gel electrophoresis and electrophoretically transferred onto polyvinylidene difluoride membranes. After blocking non-specific binding with 0.5% non-fat milk, the membranes were incubated overnight at 4°C with the same anti-nesfatin-1 and anti-H1-R antisera. The membrane was repeatedly washed and then incubated with IgG secondary antibodies. Immunopositive bands were visualized on Hyperfilm (GE Healthcare Bioscience, Piscataway, NJ, USA) using enhanced chemiluminescence.

In mice, hypothalamic preparations were homogenized in sample buffer, separated by centrifugation and the supernatant was boiled for 4 min. The total protein content of the tissue was measured using the Bradford method. Equal amounts of total protein were resolved by electrophoresis on 8% sodium dodecyl sulfate–polyacrylamide gels and then electrophoretically transferred onto polyvinylidene difluoride membranes (Bio-Rad Laboratories). Non-specific binding on the membranes was blocked with 5% non-fat milk for 1 h, and then the membranes were incubated overnight with primary antibodies at 4°C followed by secondary antibody for 1 h at 20°C. The primary antibody was polyclonal rabbit anti-human nesfatin-1 (with specificity for rat and mouse nesfatin-1; LifeSpan Bioscience Inc., Seattle, WA, USA). Nesfatin-1 was detected using enhanced chemiluminescence (Amersham Life Sciences, Arlington Heights, IL, USA). Each protein was measured using Quantity One imaging software (Bio-Rad).

Statistics

Data are expressed as means ± SEM. Statistical significance was evaluated using a two-way analysis of variance (ANOVA) followed by the Scheffé test for *post hoc* comparisons. The level of significance for all tests was established at $p < 0.05$.

Results

Effect of FMH on subsequent nesfatin-1-induced suppression of food intake and effect of nesfatin-1 on t-MH content in rat hypothalamus

The i.v.t. administration of nesfatin-1 significantly decreased food intake for 4 h compared with PBS and FMH partially attenuated this decrease (both $n = 6$ per group, $p < 0.05$). In contrast, FMH alone did not affect cumulative food intake compared with the control (Fig. 1a). Nesfatin-1 increased the pargyline-induced accumulation of t-MH in the PVN, VMH, and TMN, but not in the LH, compared with PBS ($n = 6$ per group, $p < 0.05$; Fig. 1b). However, nesfatin-1 administered intraperitoneally did not affect either appetite (Fig. 1c) or t-MH accumulation (Fig. 1d). Moreover, plasma levels of nesfatin-1 did not significantly differ after either i.v.t. or i.p. administration (Fig. 1e). Immunohistochemical analysis of double-labeled neurons revealed very few nesfatin-1-positive fibers projecting into to histamine neurons in the TMN (2.4 ± 0.5%; Fig. 1f), whereas nesfatin-1-positive neurons were detected in the PVN (Fig. 1g). These findings suggested that few nesfatin-1 neurons localized in the PVN directly activate histamine neurons in the TMN.

Effect of α-helical CRH pre-treatment on nesfatin-1-induced suppression of food intake and effect of nesfatin-1 infusion on CRH and t-MH contents in rat hypothalamus

Both 10 and 50 ng of α-helical CRH attenuated the nesfatin-1-induced suppression of food intake ($n = 6$ per group, $p < 0.05$), whereas α-helical CRH alone did not alter feeding behavior compared with PBS (Fig. 2a). Nesfatin-1 significantly increased CRH content in the PVN compared with PBS ($n = 6$ per group, $p < 0.05$; Fig. 2b). Nesfatin-1 also increased pargyline-induced t-MH accumulation in the PVN, VMH, and TMN, but not in the LH, and α-helical

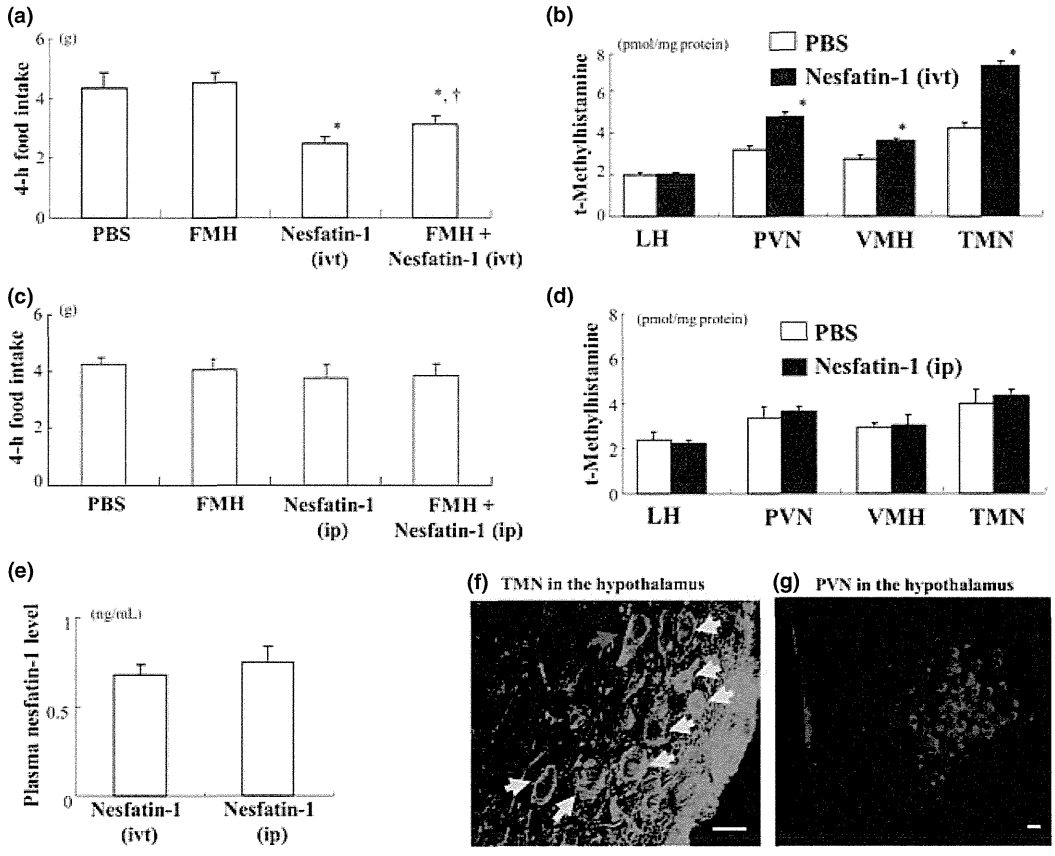

Fig. 1 Food intake at 4 h after intracerebroventricular (i.v.t.; a) and intraperitoneal (i.p.; c) administration of phosphate-buffered saline (PBS), α-fluoromethyl histidine (FMH), nesfatin-1, or FMH followed by nesfatin-1. Hypothalamic tele-methylhistamine content after i.v.t. (b) or i.p. (d) infusion of PBS or nesfatin-1, FMH + nesfatin-1, and FMH followed by nesfatin-1. Plasma nesfatin-1 levels after i.v.t. or i.p. administration of nesfatin-1 (e). $*p < 0.05$ versus PBS and FMH; $^{\dagger}p < 0.05$ versus nesfatin-1 (i.v.t.). Immunohistochemical staining for nesfatin-1 (red) in histaminergic neurons (green; yellow arrows) in the tuberomammillary nucleus (TMN) (f). Very few histamine neurons are co-localized with nesfatin-1-positive fibers (blue arrow). Immunohistochemical staining for nesfatin-1 in the paraventricular nucleus (PVN) (g). Scale bar, 10 μm.

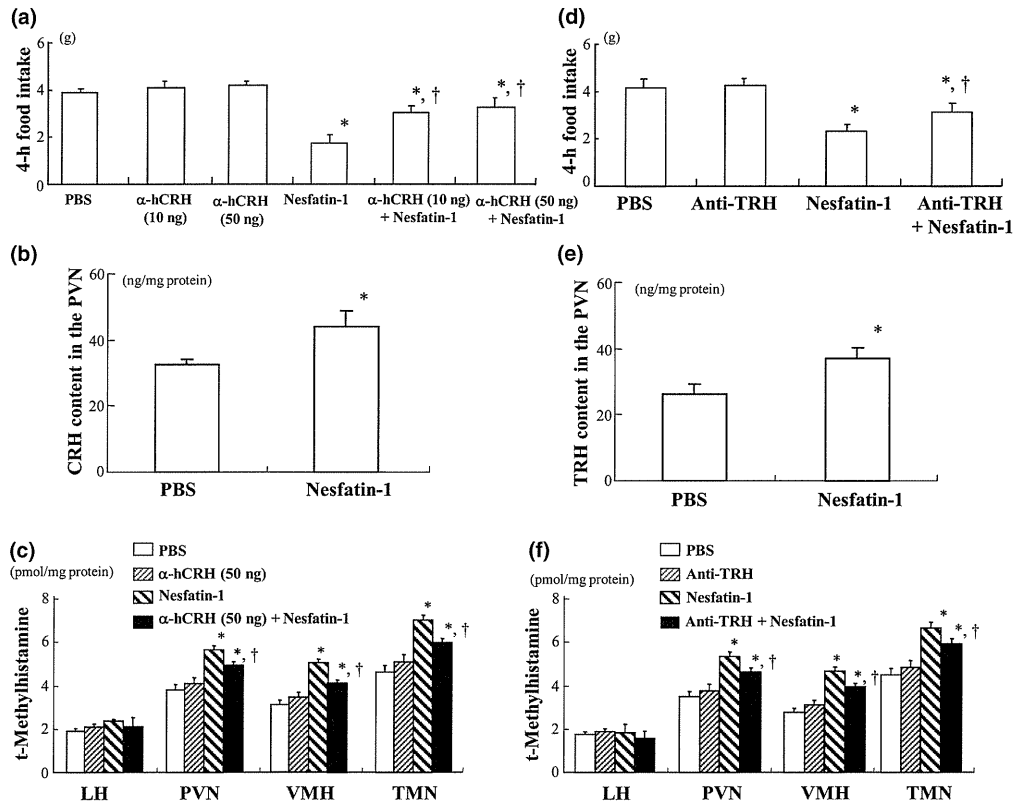

Fig. 2 Food intake at 4 h after central administration of phosphate-buffered saline (PBS), α-helical corticotropin-releasing hormone (CRH), nesfatin-1, or α-helical CRH followed by nesfatin-1 (a). $*p < 0.05$ versus PBS and α-helical CRH; $^{\dagger}p < 0.05$ versus nesfatin-1. Contents of CRH in hypothalamus after central infusion of PBS or nesfatin-1 (b). $*p < 0.05$ versus PBS. Hypothalamic t-MH content after central administration of PBS, α-helical CRH, nesfatin-1, or α-helical CRH followed by nesfatin-1(c). $*p < 0.05$ versus PBS and α-hCRH; $^{\dagger}p < 0.05$ versus nesfatin-1. Food intake at 4 h after central administration of PBS, anti-thyrotropin-releasing hormone (TRH), nesfatin-1, or anti-TRH followed by nesfatin-1 (d). $*p < 0.05$ versus PBS and anti-TRH, $^{\dagger}p < 0.05$ versus nesfatin-1. Hypothalamic TRH content after central infusion of PBS or nesfatin-1 (e). $*p < 0.05$ versus PBS. Hypothalamic t-MH content after central administration of PBS, anti-TRH, nesfatin-1, or anti-TRH followed by nesfatin-1 (f). $*p < 0.05$ versus PBS and anti-TRH; $^{\dagger}p < 0.05$ versus nesfatin-1. α-hCRH, α-helical CRH.

CRH attenuated this effect ($n = 6$ per group, $p < 0.05$; Fig. 2c).

Anti-TRH antiserum diminished the subsequent nesfatin-1-induced appetite loss like CRH ($n = 6$ per group, $p < 0.05$), but did not affect food intake alone (Fig. 2d). Nesfatin-1 increased the TRH content in the PVN compared with PBS ($n = 6$ per group, $p < 0.05$; Fig. 2e). Moreover, nesfatin-1 elevated pargyline-induced t-MH accumulation in the PVN, VMH, and TMN, but not in the LH, and prior loading with anti-TRH antiserum attenuated this effect ($n = 6$ per group, $p < 0.05$; Fig. 2f).

Attenuation of the anorexic effect of nesfatin-1 in H1KO mice

The lvt administration of nesfatin-1 led to approximate 40% and 25% reductions in food intake by wild-type and H1KO mice, respectively, within 4 hours (both $n = 6$ per group, $p < 0.05$; Fig. 3).

Effect of histamine infusion on nesfatin-1 content in rat hypothalamus

Histamine significantly increased nesfatin-1 contents in the PVN, but not in the LH, VMH, or TMN of the rat hypothalamus compared with PBS ($n = 6$ per group, $p < 0.05$; Fig. 4a). The effects of histamine and PBS on plasma nesfatin-1 levels did not significantly differ (Fig. 4b).

Differential hypothalamic nesfatin-1 expression in wild-type and H1KO mice

Nesfatin-1 expression in the hypothalamus was significantly decreased in H1KO, compared with wild-type mice ($n = 6$ per group, $p < 0.05$; Fig. 4c).

Immunohistochemical staining for nesfatin-1 and H1-R in the PVN

Immunohistochemical analysis of double-labeled neurons revealed several nesfatin-1-positive neurons expressing

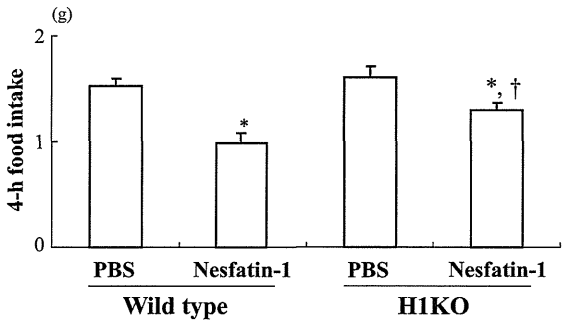

Fig. 3 Food intake 4 h after central administration of phosphate-buffered saline (PBS) or nesfatin-1 in wild-type and H1KO mice. $^{*}p < 0.05$ versus PBS (wild type and H1KO); $^{\dagger}p < 0.05$ versus nesfatin-1 (wild type).

H1-R in the PVN (Fig. 5a–c). We pre-absorbed the antibodies with purified nesfatin-1 and H1-R protein to examine their specificity. The immunohistochemical findings showed significantly less antibody labeling compared with the absence of absorption (Fig. 5d–g). Moreover, labeling specificity was controlled by omitting the nesfatin-1 and H1-R antibodies (Fig. 5h and j). Figure 5k shows the semi-quantitative findings of nesfatin-1 immunolabeling after pre-absorption with nesfatin-1 protein. With increasing concentrations of recombinant nesfatin-1 protein relative to primary antibody (1 : 1, 1 : 5, and 1 : 10 molar ratio of nesfatin-1 antibody concentration to recombinant protein concentration), nesfatin-1 immunolabeling was decreased significantly compared with immunolabeling using the primary antibody alone. The staining intensity of the anti-nesfatin-1 antibody signal for nesfatin-1 protein was linearly reduced up to fivefold the molar ratio of antigen to antibody. Pre-absorption with H1-R peptide yielded similar results (Fig. 5l). Moreover, an immunopositive band was evident at the predicted molecular weight of full length NUCB2 (50 kDa), the nesfatin-1 ($\sim$10 kDa) and H1-R ($\sim$57 kDa) proteins, indicating that the respective primary antibodies recognized nesfatin-1 and H1-R (Fig. 5m).

Discussion

Nesfatin-1, CRH, TRH, and hypothalamic neuronal histamine exert anorexigenic effects in the hypothalamus, but their functional relationships are not clear, particularly those between nesfatin-1 and histamine. Our results showed that FMH-induced depletion of neuronal histamine or H1-R deficiency partially attenuated the subsequent nesfatin-1-induced suppression of food intake. These findings indicate that endogenous neuronal histamine and associated H1-R partially mediate the anorexigenic effect of nesfatin-1. Thus, understanding how nesfatin-1 affects hypothalamic neuronal histamine levels is important. After release from nerve terminals, histamine is rapidly converted into the metabolite, t-MH, which is then deaminated, indicating that more information is generated about histamine by measuring metabolite concentrations than by measuring histamine itself. Pargyline, a monoamine oxidase B inhibitor, induces t-MH accumulation in extraneuronal spaces (Oishi *et al.* 1987). We showed that nesfatin-1 increased t-MH levels in the PVN, VMH, and TMN, but not in the LH. However, very few nesfatin-1-positive fibers projected into histamine neurons, suggesting that nesfatin-1 indirectly activates histamine neurons. Furthermore, we found that nesfatin-1 increased the CRH and TRH contents in the PVN, suggesting that nesfatin-1 increases histamine turnover, synthesis and release in the hypothalamus via CRH and/or TRH neurons in the PVN.

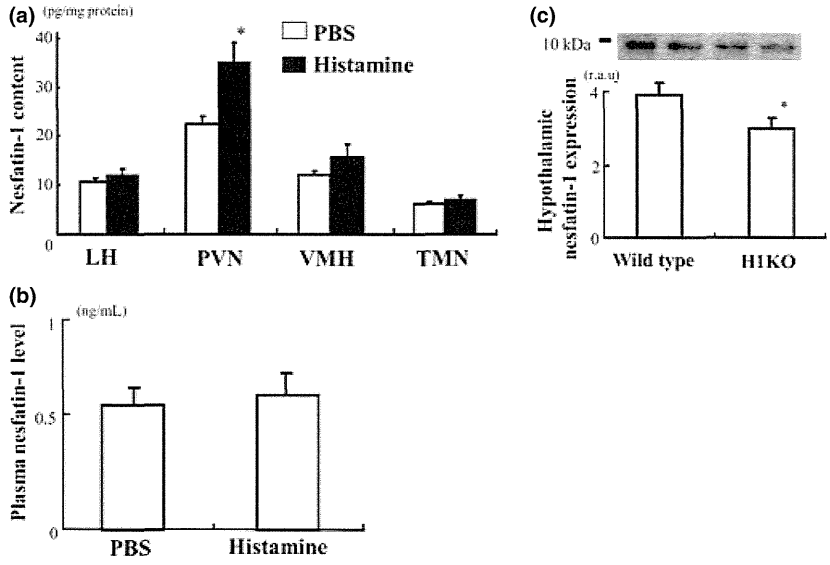

Fig. 4 (a and b): Nesfatin-1 content in the hypothalamus (a) and plasma nesfatin-1 levels (b) after central infusion of phosphate-buffered saline (PBS) or histamine. $^{*}p < 0.05$ versus PBS. (c) Nesfatin-1 expression in the hypothalamus in wild type and H1KO mice. $^{*}p < 0.05$ versus wild-type mice.

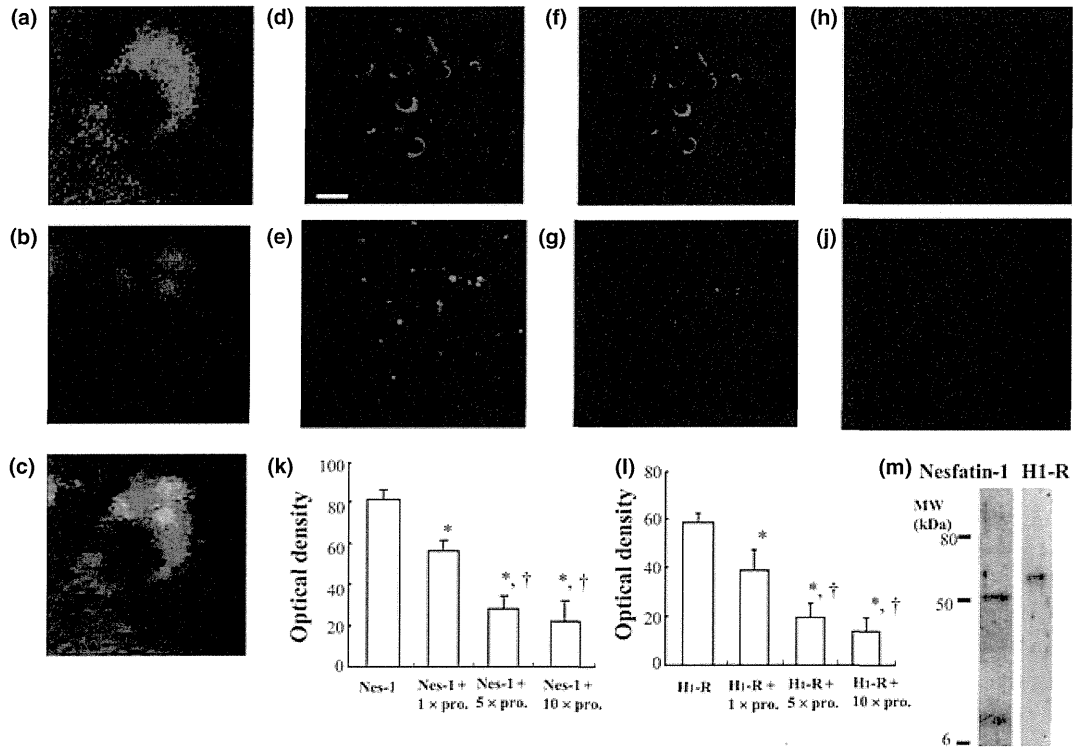

Fig. 5 Nesfatin-1 neurons (red) express H1-Rs (green) (a–c). Nesfatin-1 or H1-R antibody pre-absorbed without (d and e) or with (f and g) 1× nesfatin-1 or H1-R protein. Signals are undetectable after substituting nesfatin-1 or H1-R antibodies with normal serum and incubation with secondary antibody for staining with primary antibodies (h and j). Scale bar, 10 μm. Bar graph shows intensity of nesfatin-1 and H1-R labeling with and without nesfatin-1 and H1-R recombinant protein at 1 : 1 (×1 pro.), 1 : 5 (×5 pro.), and 1 : 10 (×10 pro.) molar concentrations of nesfatin-1 or H1-R antibodies (k and l). Values in graph represent mean total immunolabeling; $^{*}p < 0.05$ versus nesfatin-1 or H1-R; $^{\dagger}p < 0.05$ versus nesfatin-1 + 1 × 1 pro. or H1-R + 1 × 1 pro. Nes-1 means nesfatin-1. Pro. means protein. (m) Western blots show that nesfatin-1 and H1-R antibodies detected NUCB2 (~50 kDa), nesfatin-1 (~10 kDa), and H1-R (~57 kDa) proteins, respectively.

A recent study has shown that nesfatin-1 influences the activity of a large proportion of PVN neurons, including those containing CRH and TRH *in vitro* (Price *et al.* 2008). Because the activation of brain CRH and TRH signaling pathways inhibits food intake (Kow and Pfaff 1991; Richard *et al.* 2000), we investigated whether endogenous CRH or TRH activation mediated the central action of nesfatin-1 on food intake. We demonstrated that a central nesfatin-1 infusion increased CRH and TRH levels in the PVN of the hypothalamus. The central administration of α-helical CRH and anti-TRH attenuated the nesfatin-1-induced reduction in food intake, suggesting that CRH and TRH mediate the anorectic effect of nesfatin-1 in the hypothalamus.

Our results provide insight into the relationships among CRH, TRH, and neuronal histamine. We previously demonstrated that CRH- and TRH-induced increases in histamine turnover are suppressed by α-helical CRH and anti-TRH pretreatment, respectively. Moreover, CRH1-Rs and TRH type 2 receptors (TRH2-Rs) are expressed on the cell bodies of histamine neurons in the TMN (Gotoh *et al.* 2005, 2007). Thus, we speculated that nesfatin-1 signaling regulates neuronal histamine via CRH and/or TRH. Our results support this hypothesis because α-helical CRH and anti-TRH attenuated the subsequent nesfatin-1-induced increase in hypothalamic histamine turnover. We demonstrated that nesfatin-1 suppressed food intake by activating histamine neurons in the TMN via CRH and TRH neurons, which supports the finding that 20–30% of PVN nesfatin-1 cells synthesize TRH and that a subpopulation of about 20% of nesfatin-1 PVN neurons co-express CRH, which inhibits food intake (Stengel *et al.* 2010). Nesfatin-1 was found to act centrally to reduce dark-phase food intake through CRH pathways, using the non-selective CRH antagonist, astressin B; however, α-helical CRH diminished nesfatin-1-induced hypophagia (Stengel *et al.* 2009a). These data support our finding that the nesfatin-1-induced appetite loss involves TRH neurons. The mechanism underlying this discrepancy is not clear, but one possible explanation is that it is due to differences in pharmacological mechanism between these CRH antagonists.

Here, essential questions can be raised as to why hyperphagia was not evident in rats depleted of histamine

by FMH and why food intake did not differ between wild-type and H1KO mice. A definite answer to the query has not yet been proposed. However, these results are compatible with the findings that histamine depletion by FMH does not affect daily food intake, and that H1KO mice tended to consume more basal food than in wild-type mice; but this effect was not significant (Yoshimatsu *et al.* 1999; Mollet and Lutz 2001). One possible explanation is that the differences in mean daily food intake between PBS and FMH administration as well as between wild-type and H1KO mice are relatively small compared with the deviation of daily food intake in both groups. In addition, neither α-helical CRH nor anti-TRH alone increased food intake. These results are also compatible with those of others showing that α-helical CRH attenuates the leptin-induced reduction of food intake although a single administration of α-helical CRH does not significantly affect food consumption, and TRH as well as a TRH-R deficiency does not affect feeding behavior (Yamada *et al.* 1997; Uehara *et al.* 1998; Zeng *et al.* 2007; Sun *et al.* 2009). A higher dose of α-helical CRH and anti-TRH might have resulted in significantly less food intake compared with a control group as well as a more sustained attenuation of the anorexigenic effect of nesfatin-1.

Finally, we examined whether neuronal histamine activated nesfatin-1 neurons. We showed that histamine activates nesfatin-1 neurons in the PVN, suggesting that histamine neurons may activate some nesfatin-1 neurons via CRH and TRH release. Others have shown that central leptin administration activates CRH and TRH neurons and increases histamine turnover in the hypothalamus (Yoshimatsu *et al.* 1999; Nillni *et al.* 2000). Leptin-induced suppression of food intake is attenuated in rats pre-treated with FMH, which depletes neuronal histamine, and in H1KO mice that lack H1-R (Yoshimatsu *et al.* 1999). Moreover, we previously demonstrated that CRH directly mediated the effect of leptin signaling on neuronal histamine turnover and TRH stimulated histamine neurons (Gotoh *et al.* 2005, 2007). Furthermore, the results of this study showed that nesfatin-1 administration activates CRH, TRH, and histamine neurons, all of which are involved in the regulation of leptin in the hypothalamus. However, leptin does not appear to be a modulator of NUCB2 and nesfatin-1 expression in hypothalamic nuclei (Oh-I *et al.* 2006; Garcia-Galiano *et al.* 2010). This observation confirms the suggestion that nesfatin-1 has a leptin-independent mode of action (Shimizu *et al.* 2009). Thus, we speculated that the anorexigenic action of nesfatin-1 is mediated by CRH, TRH, and neuronal histamine via leptin-independent pathways, although a leptin to CRH, TRH, and neuronal histamine signaling cascade exists (Gotoh *et al.* 2005, 2007).

Nesfatin-1 is synthesized in several areas of the hypothalamus, including the PVN, VMH, ARC, and LH, where it co-localizes with neurotransmitters/neuropeptides (Oh-I *et al.* 2006; Brailoiu *et al.* 2007; Foo *et al.* 2008; Fort *et al.* 2008). These hypothalamic nuclei play important roles in the regulation of energy metabolism, and they contain receptors that signal nutritional status, including leptin levels (Mercer *et al.* 1996). Far less is known about the role of nesfatin-1 in the LH. The LH has often been referred to as a feeding center because lesions in this region result in hypophagia and weight loss (Anand and Brobeck 1951). The LH contains cells that synthesize melanin-concentrating hormone (MCH) and orexin, both of which are orexigenic factors (Date *et al.* 1999). We found that the central administration of histamine increased nesfatin-1 content in the PVN, but not in the LH, suggesting that nesfatin-1 does not act in the LH to regulate feeding behavior. This finding is not consistent with a previous study showing that about 80% of the nesfatin-1-positive neurons were double labeled with MCH (Fort *et al.* 2008). Co-expression of nesfatin-1 and MCH suggests a complex physiological relationship because nesfatin-1 induces satiety (Oh-I *et al.* 2006), whereas MCH stimulates the appetite (Pissios *et al.* 2006). Moreover, the central administration of nesfatin-1 increases orexin mRNA expression in fed goldfish, but decreases it in unfed goldfish, suggesting that the effect of nesfatin-1 on brain expression of peptides that regulate appetite might may depend on feeding status (Kerbel and Unniappan 2012). Considering the opposing anorectic and orexigenic actions of nesfatin-1 and MCH, nesfatin-1

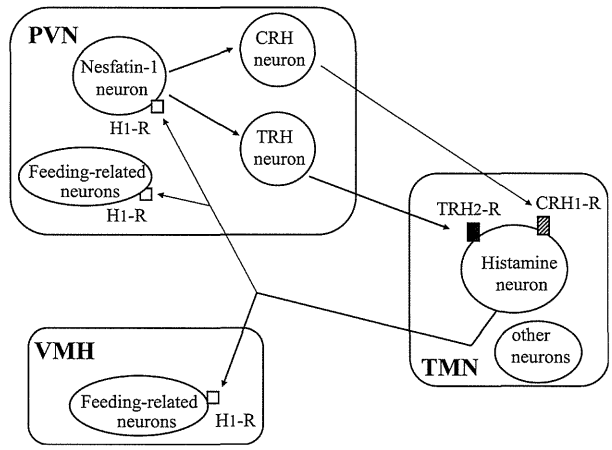

Fig. 6 Proposed model for interactions among nesfatin-1, corticotropin-releasing hormone (CRH), thyrotropin-releasing hormone (TRH), and histamine neurons in regulation of food intake. Nesfatin-1 neurons in paraventricular nucleus (PVN) regulate tuberomammillary nucleus (TMN) histamine neurons via CRH and/or TRH neurons for which receptors are expressed on the histamine neurons. Neuronal histamine directly suppresses food intake via H1-R, which is expressed on neurons (including nesfatin-1 neurons) in the ventromedial nucleus (VMH) and PVN that are related to feeding. Such neurons produce peptides such as BDNF and NPY or co-localize with H1-R and influence feeding behavior.

might modulate the effect of MCH in integrative feeding behavior.

Intraperitoneal and subcutaneous routes of nesfatin-1 administration suppress food intake and thus, peripheral nesfatin-1 probably crosses the blood–brain barrier (BBB) and acts in the hypothalamus to regulate energy metabolism and appetite (Shimizu *et al.* 2009). Nesfatin-1 has been detected in rat serum (but its origin remains unknown) and in rat gastric mucosa (Stengel *et al.* 2009b). Furthermore, nesfatin-1-immunoreactive cells co-localize with insulin in pancreatic islets (Gonzalez *et al.* 2009) implying that centrally infused nesfatin-1 might leak into the periphery via the venous system. Our results showed that the central administration of a single dose of nesfatin-1 at a concentration too low to exert effects when delivered peripherally immediately suppressed feeding behavior. We found no significant difference in plasma nesfatin-1 levels after the i.v.t. and i.p. administration of nesfatin-1. These findings support that the dose of peripherally administered nesfatin-1 required to reduce food intake is about 1000-fold higher than effective dose of centrally treated nesfatin-1 (Stengel *et al.* 2010).

We developed a working model of the feeding and satiety neuronal network via signaling between nesfatin-1 and histamine (Fig. 6). Nesfatin-1 might act on CRH and TRH neurons in the PVN, and then activated CRH and TRH neurons might in turn regulate histamine neurons in the TMN of the hypothalamus through CRH1-R and TRH2-R, respectively. Furthermore, we suggest that neuronal histamine stimulates nesfatin-1 neurons in the PVN directly via H1-R. This study provides novel insight into the action of nesfatin-1 in the hypothalamic regulation of energy metabolism.

Acknowledgments

This study was supported by a grant for Research on Measures for Intractable Diseases from Japan's Ministry of Health, Labour, and Welfare. The authors do not have any conflicting or competing interests.

References

Anand B. K. and Brobeck J. R. (1951) Localization of a "feeding center" in the hypothalamus of the rat. *Proc. Soc. Exp. Biol. Med.* **77**, 323–324.

Berthoud H. R. and Morrison C. (2008) The brain, appetite, and obesity. *Annu. Rev. Psychol.* **59**, 55–92.

Brailoiu G. C., Dun S. L., Brailoiu E., Inan S., Yang J., Chang J. K. and Dun N. J. (2007) Nesfatin-1: distribution and interaction with a G protein-coupled receptor in the rat brain. *Endocrinology* **148**, 5088–5094.

Date Y., Ueta Y., Yamashita H., Yamaguchi H., Matsukura S., Kangawa K., Sakurai T., Yanagisawa M. and Nakazato M. (1999) Orexins, orexigenic hypothalamic peptides, interact with autonomic, neuroendocrine and neuroregulatory systems. *Proc. Natl Acad. Sci. USA* **96**, 748–753.

Elmquist J. K., Coppari R., Balthasar N., Ichinose M. and Lowell B. B. (2009) Identifying hypothalamic pathways controlling food intake, body weight, and glucose homeostasis. *J. Comp. Neurol.* **493**, 63–71.

Foo K. S., Brismar H. and Broberger C. (2008) Distribution and neuropeptide coexistence of nucleobindin-2 mRNA/nesfatin-like immunoreactivity in the rat CNS. *Neuroscience* **156**, 563–579.

Fort P., Salvert D., Hanriot L., Jego S., Shimizu H., Hashimoto K., Mori M. and Luppi P. H. (2008) The satiety molecule nesfatin-1 is co-expressed with melanin concentrating hormone in tuberal hypothalamic neurons of the rat. *Neuroscience* **155**, 174–181.

Franklin K. B. J. and Paxinos G. (1997) *The Mouse Brain in Stereotaxic Coordinates*. Academic Press, San Diego.

Fukagawa K., Sakata T., Shiraishi T., Yoshimatsu H., Fujimoto K., Ookuma K. and Wada H. (1989) Neuronal histamine modulates feeding behavior through H1-receptor in rat hypothalamus. *Am. J. Physiol.* **256**, R605–R611.

Garcia-Galiano D., Navarro V. M., Roa J. *et al.* (2010) The anorexigenic neuropeptide, nesfatin-1, is indispensable for normal puberty onset in the female rat. *J. Neurosci.* **30**, 7783–7792.

Goebel M., Stengel A., Wang L., Lambrecht N. W. and Tache Y. (2009) Nesfatin-1 immunoreactivity in rat brain and spinal cord autonomic nuclei. *Neurosci. Lett.* **452**, 241–246.

Gonzalez R., Tiwari A. and Unniappan S. (2009) Pancreatic beta cells co-localize insulin and pronesfatin immunoreactivity in rodents. *Biochem. Biophys. Res. Commun.* **381**, 643–648.

Gotoh K., Fukagawa K., Fukagawa T., Noguchi H., Kakuma T., Sakata T. and Yoshimatsu H. (2005) Glucagon-like peptide-1, corticotrophin-releasing hormone, and hypothalamic neuronal histamine interact in the leptin-signaling pathway to regulate feeding behavior. *FASEB J.* **19**, 1131–1133.

Gotoh K., Fukagawa K., Fukagawa T., Noguchi H., Kakuma T., Sakata T. and Yoshimatsu H. (2007) Hypothalamic neuronal histamine mediates the thyrotropin-releasing hormone-induced suppression of food intake. *J. Neurochem.* **103**, 1102–1110.

Inoue I., Yanai K., Kitamura D., Taniuchi I., Kobayashi T., Niimura K., Watanabe T. and Watanabe T. (1996) Impaired locomotor activity and exploratory behavior in mice lacking histamine H1 receptors. *Proc. Natl Acad. Sci. USA* **93**, 13316–13320.

Kennedy G. C. (1950) The hypothalamic control of food intake in rats. *Proc. R. Soc.* **137**, 535–549.

Kerbel B. and Unniappan S. (2012) Nesfatin-1 suppresses energy intake, co-localises ghrelin in the brain and gut, and alters ghrelin, cholecystokinin and orexin mRNA expression in goldfish. *J. Neuroendocrinol.* **24**, 366–377.

Kow L. M. and Pfaff D. W. (1991) The effects of the TRH metabolite cyclo (His-Pro) and its analogs on feeding. *Pharmacol. Biochem. Behav.* **38**, 359–364.

Mercer J. G., Hoggard N., Williams L. M., Lawrence C. B., Hannah L. T. and Trayhurn P. (1996) Localization of leptin receptor mRNA and the long form splice variant (Ob-Rb) in mouse hypothalamus and adjacent brain regions by in situ hybridization. *FEBS Lett.* **387**, 113–116.

Mollet A., Lutz T. A., Meier S., Riediger T., Rushing P. A. and Scharrer E. (2001) Histamine H1 receptors mediate the anorectic action of the pancreatic hormone amylin. *Am. J. Physiol. Regul. Integr. Comp. Physiol.* **281**, R1442–R1448.

Nillni E. A., Vaslet C., Harris M., Hollenberg A., Bjorbak C. and Flier J. S. (2000) Leptin regulates prothyrotropin-releasing hormone biosynthesis. Evidence for direct and indirect pathways. *J. Biol. Chem.* **275**, 36124–36133.

Oh-I S., Shimizu H., Satoh T. *et al.* (2006) Identification of nesfatin-1 as satiety molecule in the hypothalamus. *Nature* **443**, 709–712.